

UNIVERSITY OF OKLAHOMA  
GRADUATE COLLEGE

CORRELATING RATE OF PENETRATION AND BIT TRIPS TO 3D SURFACE  
SEISMIC DATA, ANADARKO SHELF, OKLAHOMA

A THESIS  
SUBMITTED TO THE GRADUATE FACULTY  
in partial fulfillment of the requirements for the  
Degree of  
MASTER OF SCIENCE

By  
JOSEPH SNYDER  
Norman, Oklahoma  
2016

CORRELATING RATE OF PENETRATION AND BIT TRIPS TO 3D SURFACE  
SEISMIC DATA, ANADARKO SHELF, OKLAHOMA

A THESIS APPROVED FOR THE  
CONOCOPHILLIPS SCHOOL OF GEOLOGY AND GEOPHYSICS

BY

---

Dr. Kurt Marfurt, Chair

---

Dr. Matthew Pranter

---

Dr. Deepak Devegowda

© Copyright by JOSEPH SNYDER 2016  
All Rights Reserved.

*For my family*

## **Acknowledgements**

First, I would like to thank the ConocoPhillips School of Geology & Geophysics for the opportunity to attain my Master of Science in Geophysics. I would like to recognize my advisor Dr. Kurt Marfurt for the guidance and encouragement on not only this thesis, but for life as well. I would also like to acknowledge Dr. Matthew Pranter and Dr. Deepak Devegowda for their advice and support over the last several years.

I would like to thank Chesapeake Energy for providing the data for this thesis. I would like to recognize Stephanie Cook and their Mid-Continent team who graciously provided me with suggestions and additional data.

This research was funded through the Attribute Assisted Seismic Processing and Interpretation Consortium: Anadarko, Arcis, BGP, BHP Billiton, Lumina Geophysical, Chesapeake Energy, Chevron, ConocoPhillips, Devon Energy Corporation, Enervest, ExxonMobil, Geophysical Insights, Mexican Institute of Petroleum, Marathon Oil Corporation, Newfield Exploration, Occidental Petroleum Corporation, Petrobras, Pioneer Natural Resources, Remark Energy Technology Inc., Schlumberger, Shell, SM Energy, and Southwestern Energy. Another major supporter in the completion of this thesis was the Mississippi Lime Consortium: Chesapeake Energy, Devon Energy Corporation, QEP Resources, and Sinopec (Tiptop Oil and Gas).

I would like to thank my friend and research partner Xuan Qi for the helping me get acclimated to geophysical research and grad school at the University of Oklahoma. I would like to thank Tao Zhao for instruction on the use of the AASPI Proximal Support Vector Machine and troubleshooting with my data. Abdulmohsen AlAli created and provided me with the seismic inversion for this project and I cannot thank him enough.

Furthermore, I would like to recognize Dr. Brad Wallet for his statistical suggestions and assistance with MATLAB code. I would also like to thank Katherine Lindzey for creating the geologic framework for this project.

As with the aforementioned people, many other students and friends at the University of Oklahoma have had an impact on my time in graduate school and my research. I would like to thank Dr. John Pigott, Thang Ha, Yuji Kim, Fangyu Li, Tengei Lin, Jie Qi, Oluwatobi Olorunsola, Lennon Infante, Megan Gunther, Alex Besov, Bobby Hardisty, Murphy Cassel, Sumit Verma, Marcus Cahoj, Alyssa Karis, Ian Stark, Jackson Haffener, April Moreno-Ward, Bryce Hutchinson, John Hornbuckle, Niles Wethington, Rae Jacobsen, Gabriel Machado, Lydia Jones, Jennifer Roberts, Sam Eccles, Deven Gibbs, Leighton Dilbeck, Riley Schultz, Ryan Branson, Grant Muncrief and Marissa Mercado.

I would like to thank Carson West, Luis Callente, Kasey Wilcox, Mireya Mendez, Ashley Porras, Julianne Persa, Emily Wellborn and Shauna Snyder – your friendships are precious to me. I am grateful for everything you do.

Finally, I would like to express the utmost gratitude to my parents, my siblings and the rest of my family for their unconditional love and support over the last 24 years. I would not be who or where I am today without you; words cannot describe how much I appreciate and love you all.

## Table of Contents

Acknowledgements .....	iv
List of Tables .....	ix
List of Figures .....	x
Abstract .....	xvi
Chapter 1: Introduction .....	1
Chapter 2: Geologic Background .....	3
Regional Geology .....	3
Local Geology .....	4
Chapter 3: Data .....	13
Data Available .....	13
Mudlogs .....	13
Chapter 4: Methods .....	17
Geometric Attributes .....	17
Geomechanical Attributes.....	17
Time to Depth Conversion.....	18
Correlation using a Support Vector Machine Training .....	19
Proximal Support Vector Machine.....	20
Artificial Neural Network .....	20
Statistics .....	21
Chapter 5: Exploratory Data Analysis.....	31
Visualization .....	31
Proximal Support Vector Machine.....	32

Five Classes .....	32
Two Classes .....	32
Artificial Neural Network .....	32
Five Classes .....	32
Two Classes .....	33
Discussion .....	33
Chapter 6: Directional Driller Analysis.....	43
Directional Driller 1 .....	43
Visualization.....	43
Proximal Support Vector Machine.....	44
Artificial Neural Network .....	44
Directional Driller 2 .....	45
Visualization.....	45
Proximal Support Vector Machine.....	45
Artificial Neural Network .....	45
Directional Driller 3 .....	46
Visualization.....	46
Proximal Support Vector Machine.....	46
Artificial Neural Network .....	46
Discussion .....	47
Chapter 7: Bit Trip Analysis .....	70
Directional Driller 1 .....	71
Visualization.....	71

Proximal Support Vector Machine.....	71
Directional Driller 3 .....	71
Visualization.....	71
Proximal Support Vector Machine.....	71
Discussion .....	72
Chapter 8: Conclusions .....	78
Recommendations for Future Work .....	78
References .....	80
Appendix A: Petrel – Time to Depth Conversion .....	83
Appendix B: AASPI – Generate Training File .....	84
Appendix C: AASPI – PSVM Welllogs .....	87
Appendix D: MATLAB – Artificial Neural Network Inputs .....	90

## List of Tables

Table 1. 3D Survey Parameters. ....	15
Table 2. Basic statistics for cost of penetration of Directional Driller 1. Values to better characterize the center, spread and shape of the distribution are shown.....	51
Table 3. Basic statistics for cost of penetration of Directional Driller 2. Values to better characterize the center, spread and shape of the distribution are shown.....	58
Table 4. Basic statistics for cost of penetration of Directional Driller 3. Values to better characterize the center, spread and shape of the distribution are shown.....	65

## List of Figures

Figure 1. Map of the geologic provinces of Oklahoma. The study area is outlined in green and lies within Woods County, which is outlined in red (Johnson and Luza, 2008; modified from Northcutt and Campbell, 1995). .....	6
Figure 2. Cross section through Oklahoma running from the Hollis Basin in the south, through the Anadarko Basin and up to the Anadarko Shelf in the North (Modified from Johnson and Luza 2008). .....	7
Figure 3. Cross section through Oklahoma running from the Dalhart Basin in the west, through the Anadarko shelf to the Ozark Uplift in the East (Modified from Johnson and Luza 2008). .....	8
Figure 4. Paleogeographic map during the Paleozoic Mississippian (345 Ma). The red star shows the approximate location of the study area (Modified from Blakey, 2014). ...	9
Figure 5. A map displaying the Mississippian Period rock types deposited when shallow-water seas covered Oklahoma (Johnson and Luza, 2008). .....	10
Figure 6. A map displaying the carbonate facies of the Anadarko Shelf. Our study area contains majority middle ramp facies (Modified from Koch et al., 2014; Lane and DeKeyser, 1980; Watney et al., 2001). .....	11
Figure 7. A stratigraphic column of the study area. Units of interest are outlined by the red box (Modified from Mazullo, 2011). .....	12
Figure 8. Amplitude time slice through the 3D survey with the wells used in this study. The yellow box is the approximate cropped section of the 3D survey used throughout this thesis. ....	14

Figure 9. An example mudlog. The suite of data shown was compiled and analyzed by the mudlogger while this well was drilled (Courtesy of WellSight Systems). ..... 16

Figure 10. A cropped amplitude volume of the 3D seismic survey in the time domain. A single well displayed that is incorrectly lined up with the seismic. ....23

Figure 11. A cropped amplitude volume of the 3D seismic survey after being converted to the depth domain. A single well is displayed and it is now correctly lined up with the seismic. ....24

Figure 12. An example of a support vector machine in 2D space. The decision boundary, separating the two classes, is displayed by the solid green line. The margins are denoted by the dashed crimson line and the support vectors are highlighted by the blue boxes (After Cortes and Vapnik, 1995). .....25

Figure 13. An example of a binary class PSVM. The upper graph is in 2D space and the decision boundary is defined by the red line. The lower picture shows a set of points in 3D space where the decision boundary is now defined by the red plane (Modified from Zhao et al. 2014). .....26

Figure 14. A sample PSVM output. In this test, the model successfully classified 25 of the 40 testing points, or about 63%. ....27

Figure 15. A generalized ANN workflow. Inputs are entered into the network where hidden neurons are defined and weights are given to each input variable. The output is compared to the targets and the neural network completes iterations until an optimal model is created (Demuth and Beale, 1993). ....28

Figure 16. A of the structure of an ANN. It is characterized by inputs, neurons, a hidden layer, variable weights and outputs (Wang, 2003). ....29

Figure 17. An output from MATLAB’s Neural Pattern Recognition toolbox. “CE” stands for Cross-Entropy and values for this example are high meaning that this is a poor output model.....	30
Figure 18. Two histograms showing the distribution (upper) and normalized distribution (lower) for cost of penetration. Both graphs are skewed right showing that the majority of the values of COP are on the lower end of the distribution. ....	34
Figure 19. Five boxplots displaying five input parameters for this study. The points are broken into 5 classes. Class 1 being the lowest COP and Class 5 being the highest COP. There is no clear separation between the five classes. ....	35
Figure 20. Five boxplots displaying the input parameters for this study. The points are broken into 2 classes. Class 1 being lower COP and Class 2 being higher COP. A visual discriminator is difficult to define. ....	36
Figure 21. Output for the 5-class PSVM. This model correctly classified 67 of the 292 testing points, or about 23%.....	37
Figure 22. Output for the 2-class PSVM. This model correctly classified 154 of the 292 testing points, or about 53%.....	38
Figure 23. Confusion matrix for the 5-class ANN. This model correctly classified about 24% of the testing points. ....	39
Figure 24. Output results for the 5-class ANN. The cross-entropy for the training, validation and testing data is about 0.78, 1.36 and 1.43, respectively. ....	40
Figure 25. Confusion matrix for the 2-class ANN. This model correctly classified about 66% of the testing points. ....	41

Figure 26. Output results for the 2-class ANN. The cross-entropy for the training, validation and testing is 0.45, 0.68 and 0.68, respectively .....42

Figure 27. Cropped amplitude slice showing the location of Directional Driller 1’s five lateral wells. ....49

Figure 28. Two histograms showing the distribution (upper) and normalized distribution (lower) for cost of penetration for Directional Driller 1. Both graphs are skewed right showing that the majority of the values of COP are on the lower end of the distribution. ....50

Figure 29. Five boxplots displaying the five input parameters for Directional Driller 1 in this study. The points are broken into 2 classes. Class 1 being low COP and Class 2 being high COP. There is more separation between the 2 classes than in the previous chapter. ....52

Figure 30. Output for the 2-class PSVM for Directional Driller 1. This model correctly classified 34 of the 40 testing points, or about 85%. ....53

Figure 31. Confusion matrix for the 2-class ANN for Directional Driller 1. This model correctly classified about 73% of the testing points. ....54

Figure 32. Output results for the 2-class ANN for Directional Driller 1. The cross-entropy for the training, validation and testing data is about 0.46, 0.73 and 0.75, respectively. ....55

Figure 33. Cropped amplitude slice showing the location of Directional Driller 2’s five lateral wells. ....56

Figure 34. Two histograms showing the distribution (upper) and normalized distribution (lower) for cost of penetration for Directional Driller 2. Both graphs are skewed right

showing that the majority of the values of COP are on the lower end of the distribution.  
.....57

Figure 35. Five boxplots displaying the five input parameters for Directional Driller 2 in this study. The points are broken into 2 classes. Class 1 being low COP and Class 2 being high COP. There is more separation between the 2 classes than in the previous chapter. ....59

Figure 36. Output for the 2-class PSVM for Directional Driller 2. This model correctly classified 28 of the 40 testing points, or about 70%. ....60

Figure 37. Confusion matrix for the 2-class ANN for Directional Driller 2. This model correctly classified about 64% of the testing points. ....61

Figure 38. Output results for the 2-class ANN for Directional Driller 2. The cross-entropy for the training, validation and testing data is about 0.45, 0.69 and 0.69, respectively. ....62

Figure 39. Cropped amplitude slice showing the location of Directional Driller 3’s seven lateral wells. ....63

Figure 40. Two histograms showing the distribution (upper) and normalized distribution (lower) for cost of penetration for Directional Driller 3. Both graphs are skewed right showing that the majority of the values of COP are on the lower end of the distribution.  
.....64

Figure 41. Five boxplots displaying the five input parameters for Directional Driller 3 in this study. The points are broken into 2 classes. Class 1 being low COP and Class 2 being high COP. There is more separation between the 2 classes than in the previous chapter. ....66

Figure 42. Output for the 2-class PSVM for Directional Driller 3. This model correctly classified 28 of the 40 testing points, or about 70%. .....67

Figure 43. Confusion matrix for the 2-class ANN for Directional Driller 3. This model correctly classified about 66% of the testing points. ....68

Figure 44. Output results for the 2-class ANN for Directional Driller 3. The cross-entropy for the training, validation and testing data is about 0.45, 0.69 and 0.69, respectively. ....69

Figure 45. Two histograms showing the distribution (upper) and normalized distribution (lower) of bit trips for the 50 horizontal wells in the survey. Class 1 corresponds to wells that had 2-5 bit trips in the lateral, while Class 2 corresponds to wells that had 6-9 bit trips in the lateral. ....73

Figure 46. Eight boxplots displaying the eight input parameters for Directional Driller 1 in this chapter. The points are broken into 2 classes. Class 1 being 2-5 bit trips and Class 2 being 6-9 bit trips. Visual discriminators are easily understood. ....74

Figure 47. Output for the 2-class PSVM for Directional Driller 1. This model correctly classified 37 of the 40 testing points, or about 93%. .....75

Figure 48. Eight boxplots displaying the eight input parameters for Directional Driller 3 in this chapter. The points are broken into 2 classes. Class 1 being 2-5 bit trips and Class 2 being 6-9 bit trips. Visual discriminators are easily understood. ....76

Figure 49. Output for the 2-class PSVM for Directional Driller 3. This model correctly classified 36 of the 40 testing points, or about 90%. .....77

## Abstract

While initially thought to be laterally homogeneous, operators quickly realized that unconventional resource plays can exhibit considerable geologic heterogeneity. Since this realization, 3D surface seismic analysis has played a significant role in identifying drilling hazards and sweet spots. Much less effort, however, has been invested in mapping the heterogeneity of the drilling process itself, where some zones drill faster, some slower, and still others result in costly casing trips to change the bit. Given the current low oil price, there is an increased need for efficiency and cost reduction in the drilling process. A method to better predict drilling speed could make a significant impact.

In this thesis, I correlate the rate of penetration to surface seismic measurements made over the heterogeneous Mississippi Lime resource play in Woods County, Oklahoma. 50 horizontal wells with mud logs measuring the rate of penetration (ROP) in minutes/foot fall within a 70 mi<sup>2</sup> seismic survey. Exploratory data analysis shows that geomechanical attributes of P-impedance, inverted-porosity,  $\lambda\rho$  and  $\mu\rho$  and the geometric attribute curvedness have good correlations with ROP. I then evaluate a Proximal Support Vector Machine (PSVM) and an Artificial Neural Network (ANN) to predict classifications of the speed of drilling – or cost of penetration in minutes per foot – for lateral segments of the wells. Because the objective is to develop a technique to reduce the cost of drilling, I weighted each well segment by the time it took to drill, and then defined discriminant boundaries between classes defined as equally weighted percentiles. I initially attempted to assign 40 of the wells, irrespective of driller, into 5-class and 2-class PSVM and ANN models, but obtained poor validation with the 10

wells not used in the training. Hypothesizing that a given directional drilling company will follow consistent, if not rigid, company specific operating protocols, I used these smaller data sets to generate three 2-class (fast and slow) PSVM and ANN models. I obtained increased validation of 2-class PSVM of 17-32%; however, the results for the ANN were weaker with a decrease in validation for some cases. More specifically, the 2-class PSVM correctness increased from 57% for the entire data set to 85%, 70% and 70% when the data were separated by the three directional drillers. The 2-class ANN correctness changed from 66% for the entire data set to 73%, 64% and 66% when the data were separated by directional driller.

In an effort to further lower drilling costs, I correlate bit trips in the lateral segments of wells to Gray Level Co-Occurrence Matrix (GLCM) texture attributes. Using eight GLCM attributes – contrast, correlation, dissimilarity, energy, entropy, homogeneity, mean and variance – and building off the knowledge that the directional driller had an effect on the results of the PSVM, I was able to obtain strong correctness for a 2-class (high number of bit trips and low number of bit trips) PSVM model. The 2-class PSVM correctness obtained ranged between 90-93%.

## **Chapter 1: Introduction**

The Mississippian Limestone carbonates in north-central Oklahoma have yielded stellar oil and gas reservoirs since the early 1900's (Koch et al., 2014). While wildcatters once targeted geographic structural traps, the advent of unconventional drilling and completion techniques has allowed for the exploitation of stratigraphic traps by exploration and production companies (Lindzey, 2015). This thesis strives to improve well planning and reduce drilling costs through the use of mudlogs and 3D seismic data.

In today's industry, drilling a horizontal well is one of the largest expenses of the petroleum production process. The controlling factor in the cost of drilling a well is time and the majority of the time is consumed either while drilling or making a bit trip (Bourgoyne et al., 1986). More specifically, the time can be broken down into the rotating time, nonrotating time and trip time (Bourgoyne et al., 1986). Ideally, one would like to – safely and efficiently – drill the well as quickly as possible while maximizing rotating time and minimizing nonrotating and trip time to decrease the overall cost of drilling. Drilling rate in the petroleum industry is referred to as rate of penetration and primarily depends on weight on bit, speed of bit rotation, drilling fluid flow rate, and the drilled formation (Bourgoyne et al., 1986). Values of rate of penetration used in this thesis will be in units of minutes per foot and will be referred to herein as cost of penetration or COP (Qi et al., 2016). By predicting COP values and bit trips throughout the study area, my goal is to statistically analyze the cost of the drilling process for a given well trajectory.

The basis for this thesis extends preliminary work done to predict COP by Qi et al. (2016). Juxtaposed with this thesis, some aspects remain the same; however, many changes were made in this study to further characterize the COP prediction and classification process. The two major points that remain constant between this thesis and the work done by Qi et al. (2016) are the use of the same geometric and geomechanical attributes and the use of a 2-class proximal support vector machine. The altered methods in this study differentiate the thesis. Data sampling in this project was defined to be that of the seismic bin size, in other words data samples for COP, geometric and geomechanical attributes were taken at every 110 ft, as opposed to every 2 ft. Each data 3D voxel along the well was then classified by this upscaled COP. For this study, classification was also tested using an artificial neural network which was not used in the study by Qi et al. (2016). After preliminary exploratory data analysis, wells are segmented by their respective directional driller and COP is analyzed separately. Furthermore, bit trips in the lateral segments of wells are segmented by their individual directional driller and analyzed separately.

## **Chapter 2: Geologic Background**

### **Regional Geology**

The wells and seismic survey in this study lie in the northeastern corner of Woods County, Oklahoma. Figure 1 shows the surrounding structural members and study area within Woods County. The study area is within the Anadarko Shelf and is bound by the Cimarron Arch to the west, the Anadarko Basin to the south and the Nemaha Uplift to the east. These structural elements formed primarily between the Late Cambrian and Early Pennsylvanian (Johnson and Luza, 2008). Figure 2 shows a cross section displaying structural features from southern Oklahoma up to the Anadarko Shelf in northern Oklahoma. Figure 3 shows a similar cross section; however, this figure runs from western Oklahoma through the Anadarko Shelf and to the eastern edge of the state.

Figure 4 shows the approximate location of the study area during the Mississippian Period. During the Paleozoic Mississippian (345 Ma), shallow seas covered the majority of Oklahoma (Johnson and Luza, 2008) and shallow-water carbonates were deposited (Figure 5) creating the Anadarko Shelf. Figure 6 shows the primary depositional environments during this time period – the inner, middle and outer ramp. Seven lithofacies are represented within this carbonate-ramp: argillaceous dolomitic mudstone, argillaceous dolomitic mudstone with chert nodules, clean dolomitic mudstone with chert nodules, nodular to bedded chert, autoclastic chert, autoclastic chert with clay infill and bioclastic wacke-grainstone (Watney et al. 2001).

## **Local Geology**

The stratigraphic units of interest for this study are from the Paleozoic Era.

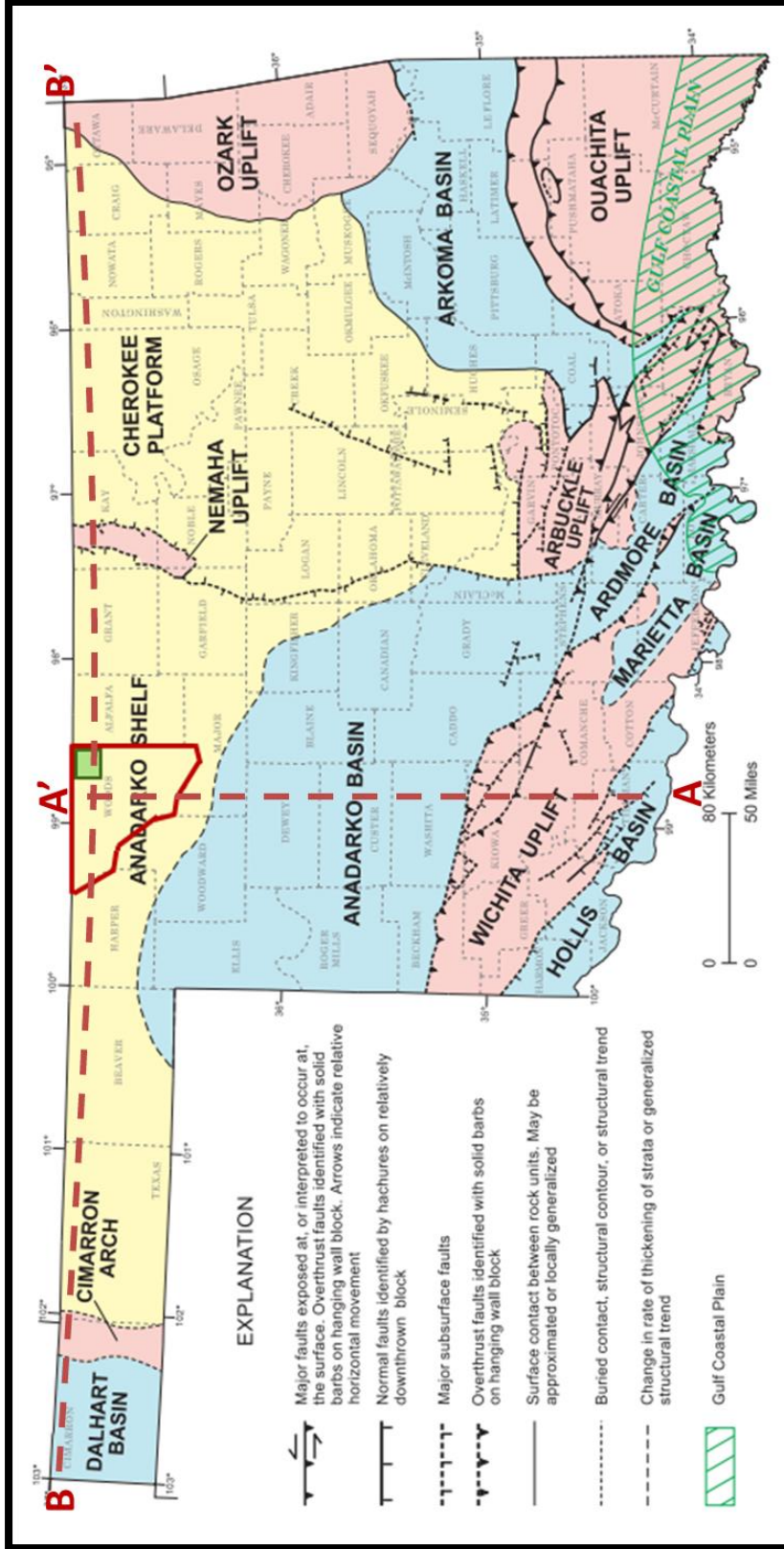
Figure 7 shows the established stratigraphic column in northeast Woods County and the series that are present in the study are the Kinderhookian, Osagean and Meramecian.

Figure 5 shows that these Mississippian rocks are primarily limestone with minor amounts of chert, sandstone and shale. Thicknesses range between 400 feet and 1,400 feet; this variability is due to erosion after the Mississippian period (Bowles Jr., 1961).

The lower portion of the Kinderhookian series is characterized by the Woodford shale which is a brown, carbonaceous, shale. The upper portion of the Kinderhookian is a sacrosic limestone that is light-gray in color (Bowles Jr., 1961). Overlying the Kinderhookian series is the Osagean series. The Osagean is primarily dolomite and limestone; however, a characteristic feature for this series is the blue-gray chert contained within (Bowles Jr., 1961). The Meramecian series overlies the Osagean. It contains dolomite with interbedded chert at the base, but becomes a gray fossiliferous limestone at the top (Bowles Jr., 1961).

The horizontal wells in the study area penetrate and produce mainly from the Osagean series – more specifically, from a section known as the Mississippi Chert or “chat.” The term “chat” is a colloquialism created by drillers due to the chattering sound the drill bit makes as it bounces off the Osagean Mississippi Chert. Subaerial exposure of the Mississippian Limestone caused porous and reworked chert to form which ranges between 50-70 feet (Bowles Jr., 1961). Chat is made through dissolution of excess amounts of calcite in meteoric waters (Rogers, 2001). Furthermore, the formation of chat is controlled by elevation and erosion; higher elevation areas allow for more

erosion to occur, regulating the distribution of carbonate that exists for later replacement by silica-saturated waters (Rogers, 2001). The Mississippi Chat is, therefore, only found in localized areas such as northeastern Woods County, Oklahoma.



**Figure 1.** Map of the geologic provinces of Oklahoma. The study area is outlined in green and lies within Woods County, which is outlined in red (Johnson and Luza, 2008; modified from Northcutt and Campbell, 1995).

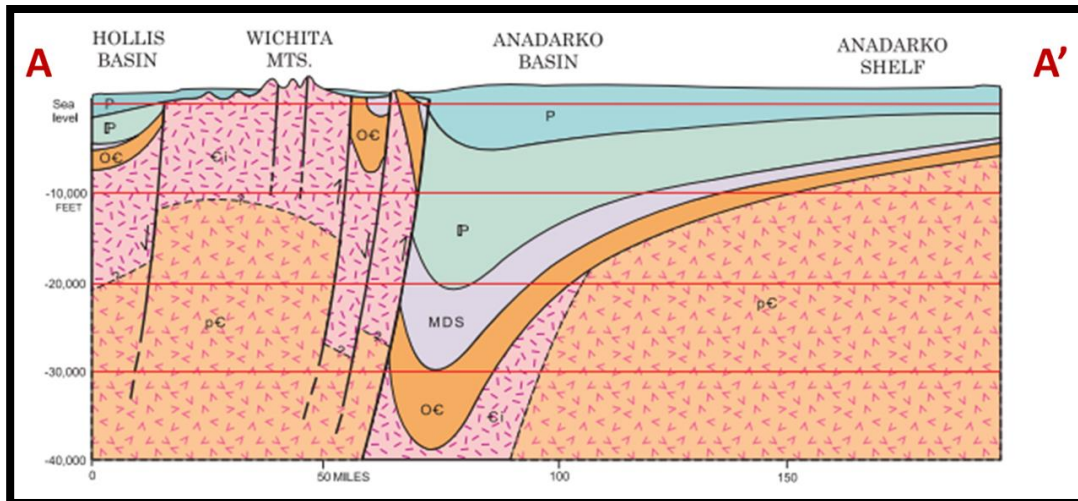


**Figure 2.** Cross section through Oklahoma running from the Hollis Basin in the south, through the Anadarko Basin and up to the Anadarko Shelf in the North (Modified from Johnson and Luza 2008).

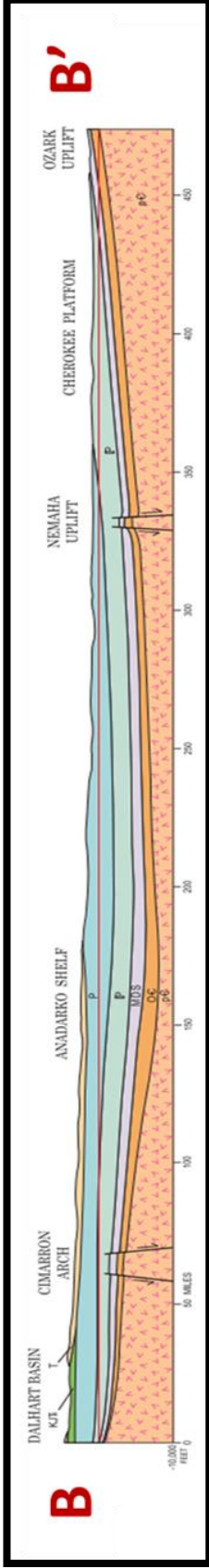


**Figure 3.** Cross section through Oklahoma running from the Dalhart Basin in the west, through the Anadarko shelf to the Ozark Uplift in the East (Modified from Johnson and Luza 2008).

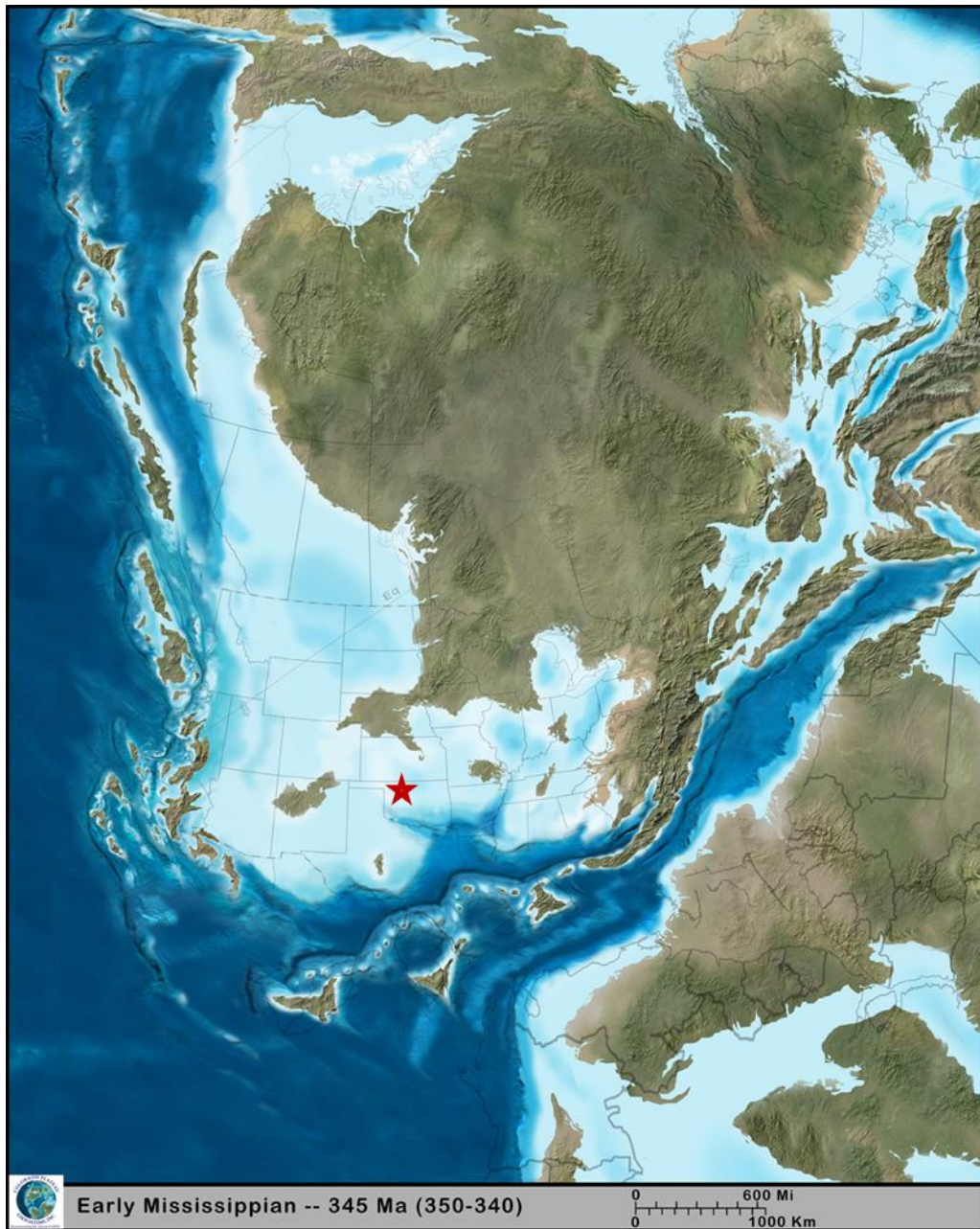


**Figure 4.** Paleogeographic map during the Paleozoic Mississippian (345 Ma). The red star shows the approximate location of the study area (Modified from Blakey, 2014).

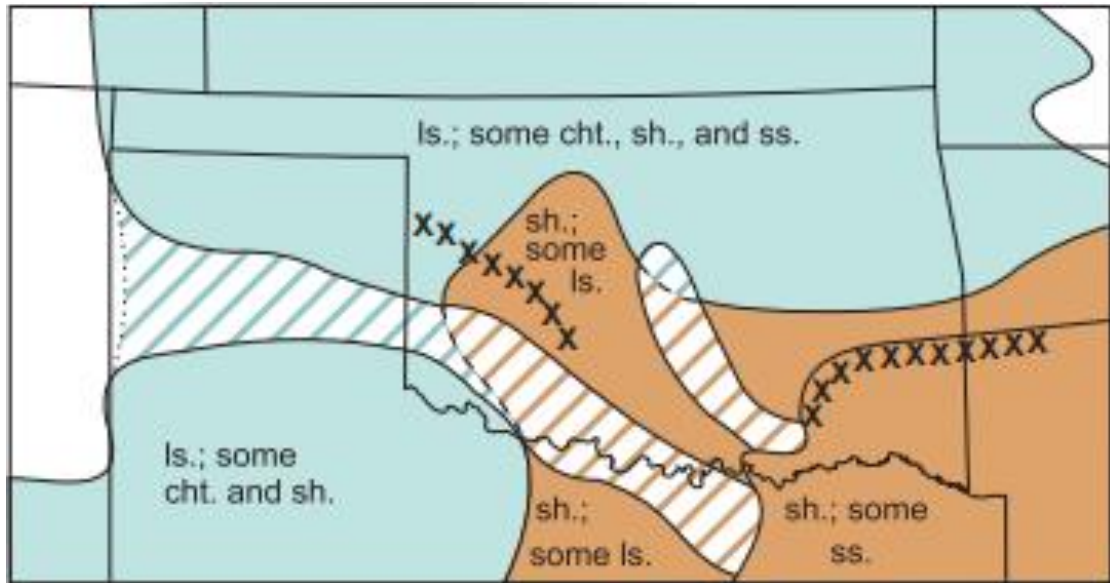


**Figure 5.** A map displaying the Mississippian Period rock types deposited when shallow-water seas covered Oklahoma (Johnson and Luza, 2008).

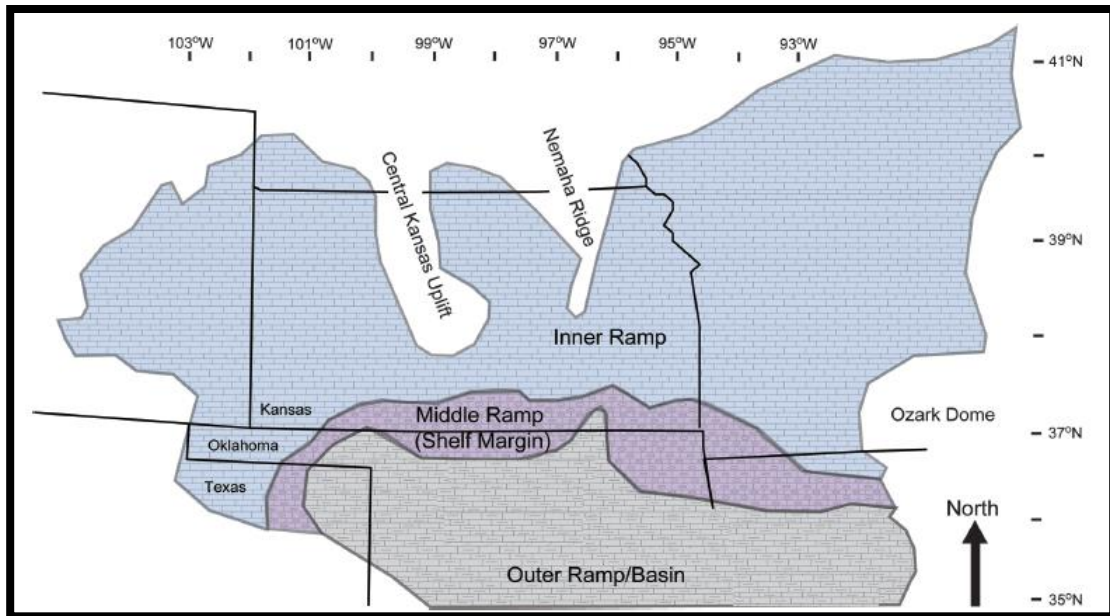


**Figure 6.** A map displaying the carbonate facies of the Anadarko Shelf. Our study area contains majority middle ramp facies (Modified from Koch et al., 2014; Lane and DeKeyser, 1980; Watney et al., 2001).

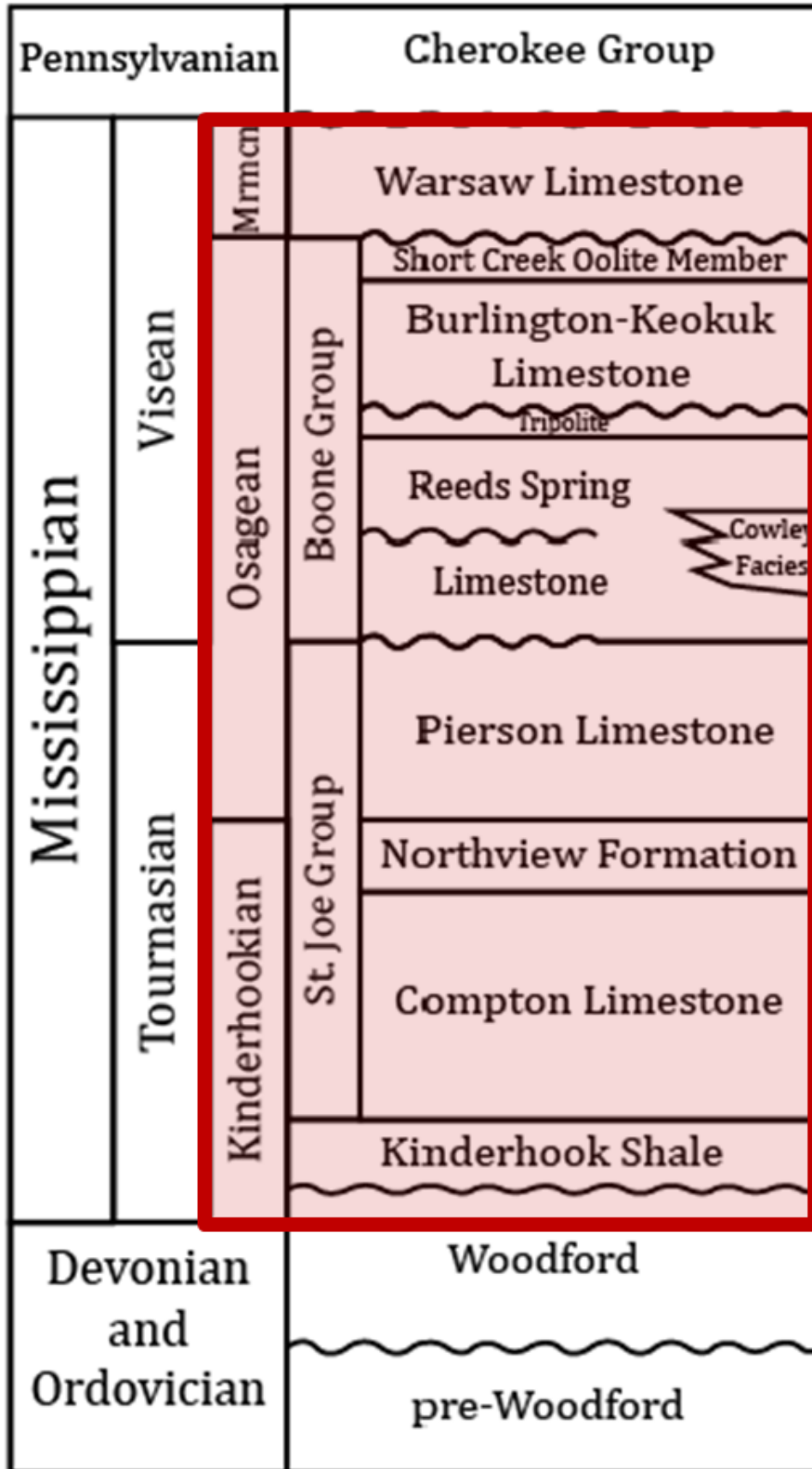


**Figure 7.** A stratigraphic column of the study area. Units of interest are outlined by the red box (Modified from Mazullo, 2011).

## **Chapter 3: Data**

### **Data Available**

The 3D Survey for this project was provided by Chesapeake Energy Corporation and was processed by Kelman Technologies in 2011. The survey is approximately 70 mi<sup>2</sup> and Figure 8 shows a time slice at the approximate Mississippian horizon through the seismic amplitude volume at t=1.02 s. The processing workflow carried out included gain recovery, spiking deconvolution, refraction statics, velocity analysis, residual statics, fxy pre-stack noise rejection, pre-stack Kirchhoff time migration, migration stretch mute, and a 6-12-80-90 Ormsby bandpass filter. Table 1 shows detailed survey parameters. The source and receiver spacing were 220 ft. The bin size was 110 ft x 110 ft with a sampling increment of 2 ms. The wavelet amplitude is laterally continuous throughout the Mississippian Limestone unit, exhibiting a high signal to noise ratio. Well data, including open-hole logs and well logs, from 50 horizontal wells and 32 vertical wells were included.

### **Mudlogs**

The mudlog was the primary piece of data used in this study. A mudlog is a suite of data analyzed and compiled during a well's drilling process by an on-site geologist better known as a mudlogger. Figure 9 shows a sample mudlog using WellSight Log Viewer courtesy of WellSight Systems. This figure shows COP, weight-on-bit, gamma ray, depth, cuttings analysis, and mud cake analysis. Every piece of data is critical to the drilling process; however, the COP values are what is crucial to this study.

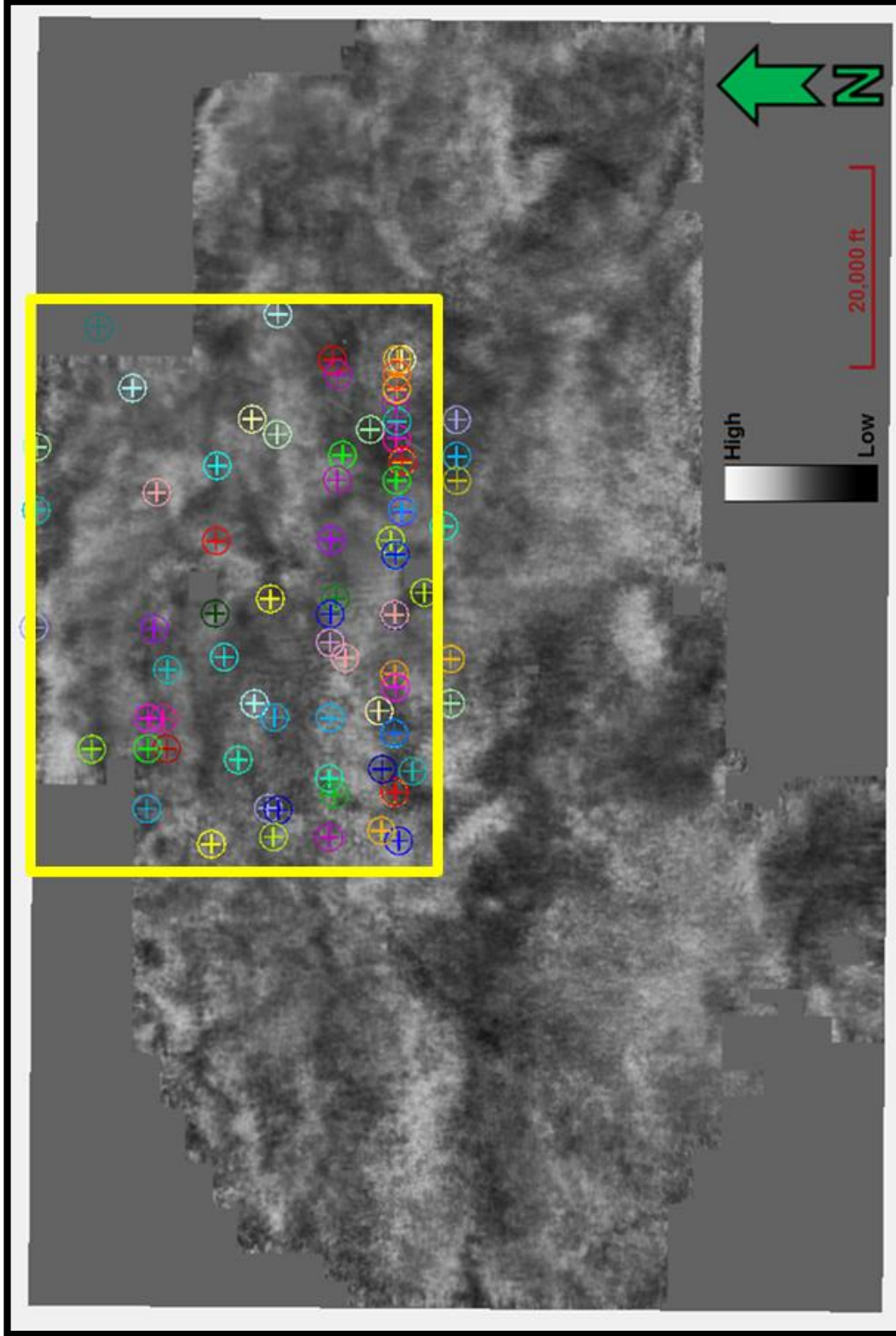


**Figure 8.** Amplitude time slice through the 3D survey with the wells used in this study. The yellow box is the approximate cropped section of the 3D survey used throughout this thesis.

Survey Parameters	
<b>County:</b>	Woods
<b>Projection:</b>	NAD27 Oklahoma North
<b>Receiver Spacing:</b>	220 ft
<b>Receiver Line Spacing:</b>	440 ft
<b>Source Spacing:</b>	220 ft
<b>Source Line Spacing:</b>	880 ft
<b>Datum:</b>	1500 ft
<b>Replacement Velocity:</b>	9000 ft/s
<b>Sample Interval:</b>	2 ms
<b>Record Length:</b>	3000 ms
<b>Azimuth:</b>	90.45°
<b>Processing Type:</b>	Post-Stack Migration
<b>Bin Size:</b>	110 ft x 110 ft

**Table 1.** 3D Survey Parameters.

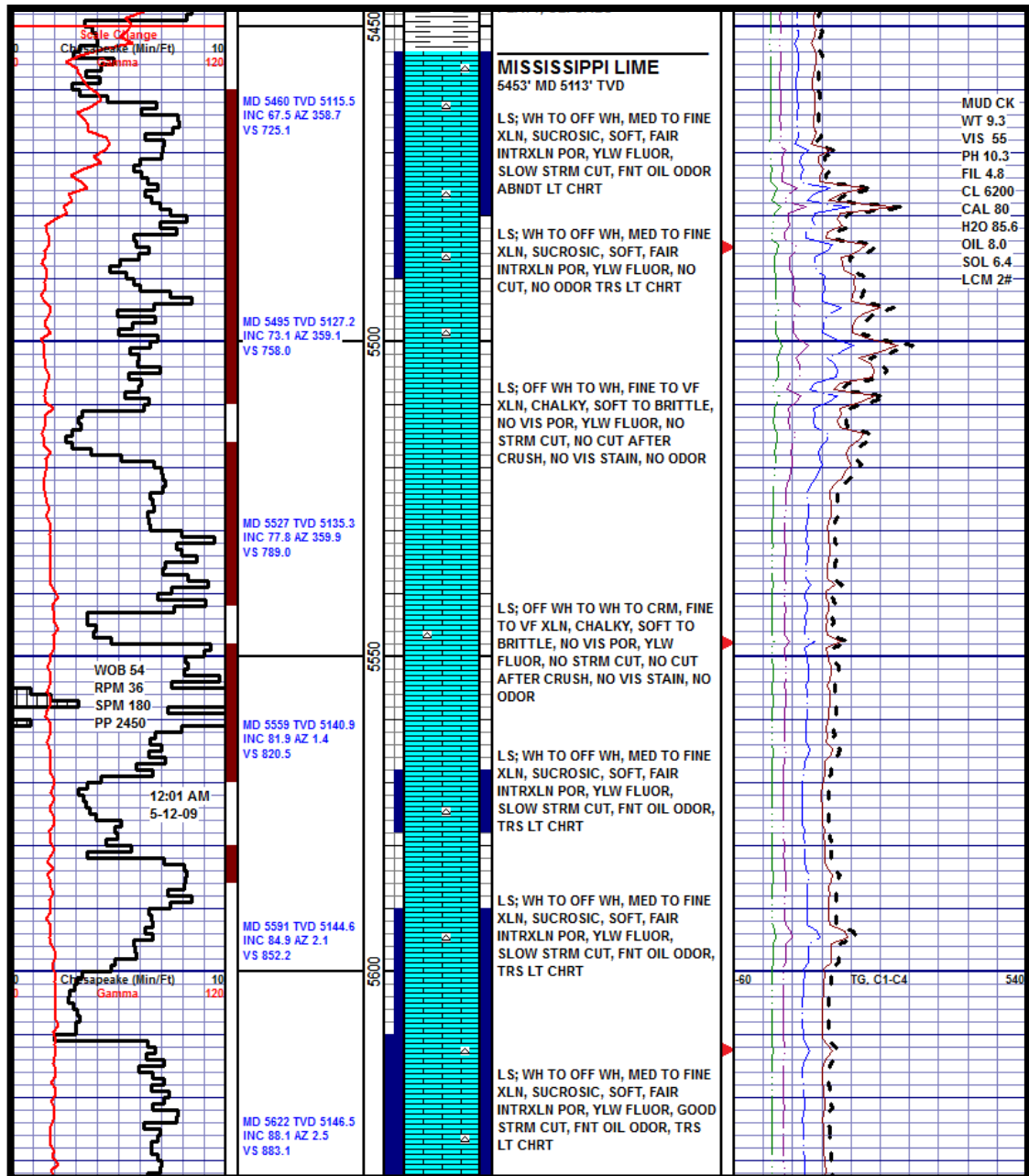


**Figure 9.** An example mudlog. The suite of data shown was compiled and analyzed by the mudlogger while this well was drilled (Courtesy of WellSight Systems).

## Chapter 4: Methods

### Geometric Attributes

I hypothesize that natural fractures either impede or facilitate the cost of penetration. Nelson (2001) finds that in addition to lithology, natural fractures are also a function of strain. Curvature, computed from 3D seismic data, is a direct measure of strain, and commonly used as a proxy for fractures (Lisle, 1994; Ghosh and Mitra, 2009). With no reason to favor most positive curvature,  $k_1$ , over most negative curvature,  $k_2$ , I combine them and use curvedness,  $C$ , defined by Chopra and Marfurt (2007) as

$$C = \sqrt{(k_1^2 + k_2^2)}, \quad (1)$$

I further hypothesize that textural homogeneity – or lack thereof – will have an effect on the ease of drilling. Texture will be analyzed through eight GLCM texture attributes – contrast, correlation, dissimilarity, energy, entropy, homogeneity, mean, variance – computed from 3D seismic data. The GLCM describes arrangements of gray levels that occur in a given space – providing quantitative texture measurements (Hall-Beyer, 2007). Gao (2004, 2007, 2009) has correlated these texture attributes to well logs using both supervised and unsupervised learning techniques.

### Geomechanical Attributes

Gong and Zhao (2007) found that brittleness of a rock affected the rate of penetration for Tunnel Boring Machines. More specifically, as rock brittleness increased, rate of penetration increased. Geomechanical attributes can aid in the analysis of brittleness, and therefore in cost of penetration analysis. A simultaneous elastic inversion is generated on this data set in order to estimate values of porosity,  $\lambda\rho$ ,

$\mu\rho$  and P-impedance using commercial software. These geomechanical attributes are used as inputs for classification as they relate to the lithology and brittleness of the drilled formation and, in turn, may have a direct effect on the COP. 16 wells with density and P-wave sonic logs are used; however, only one S-wave sonic log was available. Prior to the inversion, the data were preconditioned by applying a 10-15-110-120 Hz bandpass filter, a parabolic Radon transform and trim statics, the latter to correct for alignment errors at far offsets. Correlations between the inverted and the upscaled, measured P- and S- impedance logs at individual well locations ranged between 0.964 and 0.985 indicating a strong relationship.

### **Time to Depth Conversion**

To relate seismically derived geometric and geomechanical attributes to cost of penetration, the volumes in the time domain must be converted to the depth domain. A velocity model was created for the Mississippian Limestone using built on interpreted seismic horizons in the time domain combined with well tops picked from logs in the depth domain.

The target zone in this study is defined by the top of the Mississippian Limestone as the upper bound and the top of the Woodford Shale as the lower bound. Next, the well tops for the Mississippian Limestone and the Woodford Shale are entered as correction data. The well tops make alterations to the velocity model and create a more accurate model in the depth domain. The zone of the velocity model must next be defined. Because there is little compaction with depth for the Mississippi Lime Formation and dip was less than 2%, the velocity was chosen to be constant throughout the zone where  $V = V_0 = V_{int}$ .

The last step is to change the correction and output settings for the model. Tolerance for depth and time thickness of 60 ft and 40 ms were selected, respectively. The commercial software used disregards intervals where the difference between horizons is less than the tolerance. Surface interpolation increments of 500 ft were chosen for both X and Y. The interpolation method chosen was a moving inverse distance squared weighted average, such that closer points receive a higher weight than points further from the node.

The resulting velocity model can now be used to convert the seismically derived geometric and geomechanical attributes from time to depth. Figure 10 shows the seismic amplitude in the time domain with a well that is stretched because it is in the depth domain. Figure 11 shows the seismic after being converted to the depth domain using the new velocity model. The well fits much better and is no longer stretched. This model can now be applied to the rest of the data.

### **Correlation using a Support Vector Machine Training**

Support vector machine and artificial neural networks are both supervised learning techniques, wherein, the interpreter graphically (e.g by picking) or otherwise defines (e.g. by extracting voxel vectors about a well bore) a subset of the data that are correlated to “truth” data such as facies labels or well log measurements. In this work, the truth data will be a subset of the ROP measurements in the horizontal well logs. Voxels vectors are extracted along horizontal wellbore portions of 50 wells within the 3D survey.

## **Proximal Support Vector Machine**

Support vector machines were originally created as a means of non-linear data classification (Cortes and Vapnik, 1995). Initially used for binary classification through the use of decision-boundaries (Figure 12), SVM's have evolved into proximal support vector machines where classification is driven by the use of decision-planes (Figure 13) (Fung and Mangasarian, 2005). Support vector machines are more frequently being used as classification tools in geology and geophysics. SVM's have recently been used as a method of lithofacies classification, a means to estimate TOC from well logs, a method to map mineral prospectivity, (Zhao et al., 2014; Zhao et al., 2015; Zuo and Carranza, 2011). In this study, a PSVM will be used to classify drilling rate by analyzing the geometric and geomechanical attributes curvedness, P-impedance,  $\lambda\rho$ ,  $\mu\rho$  and inversion porosity.

To begin, a training file with a significant portion of the data is entered. Controlling parameters are chosen to define the misclassification rate and Gaussian kernel. Figure 14 shows a representative output. In this case, the application correctly classified 25 of the 40 testing points or 63% of the validation points.

## **Artificial Neural Network**

Artificial neural networks are comprised of an arrangement of variables functioning simultaneously, and are considered to be similar to the human nervous system (Demuth and Beale, 1993). ANN's are able to efficiently distinguish relationships between data that may, initially, seem to have no connection (Hsu et al., 1995). Figure 15 shows the ANN training process. Inputs are entered into the neural network where they are weighted and linked creating an output. The output is then

compared to the target output and the neural network iterates by adjusting weights of each input variable until an optimal output is found. Figure 16 shows the structure of an ANN.

I used a commercial Neural Pattern Recognition toolbox is used in this study as a means of classification for the data. The percentage of samples for the training, validation and testing steps are selected as well as the number of hidden neurons. The model is trained and iterates until the best possible result is reached. A generalized sample output is shown in Figure 17. The results for this test are poor; the cross-entropy values are too high meaning that the model is unsatisfactory.

### **Statistics**

I use the four moments of statistics-mean, variance, skewness and kurtosis as well as the median to make compare variability and consistency between three directional drillers. This suite will help to give measures of center, spread and shape for our data (Hall, 2016).

Seiler and Seiler (1989) define the first moment of statistics, mean, by

$$\bar{x} = \frac{1}{n} \sum_{i=1}^n x_i , \quad (2)$$

The mean is the arithmetic average of the data samples. Variance is the second moment and is defined by

$$\sigma^2 = \frac{1}{n-1} \sum_{i=1}^n (x_i - \bar{x})^2 , \quad (3)$$

Standard deviation, although not a moment of statistics, is important as it expresses the variability of the data in the same units as the data (Hall, 2016). It is defined as the square root of variance or

$$\sigma = \sqrt{\sigma^2} , \quad (4)$$

The variance describes how the data are distributed about the mean (Seiler and Seiler, 1989). The third moment of statistics is skewness, defined by

$$skew = \frac{1}{n} \sum_{i=1}^n \left[ \frac{x_i - \bar{x}}{\sigma} \right]^3, \quad (5)$$

and defines the asymmetry of the data about the mean (Seiler and Seiler, 1989). The fourth moment, kurtosis, measures the peakedness of a distribution of data (Seiler and Seiler, 1989) and it is defined by

$$kurt = \frac{1}{n} \sum_{i=1}^n \left[ \frac{x_i - \bar{x}}{\sigma} \right]^4 - 3, \quad (6)$$

The median is computed by first ordering the samples  $x_i$  from low to high values and then taking the middle sample of the ordered array as the result.

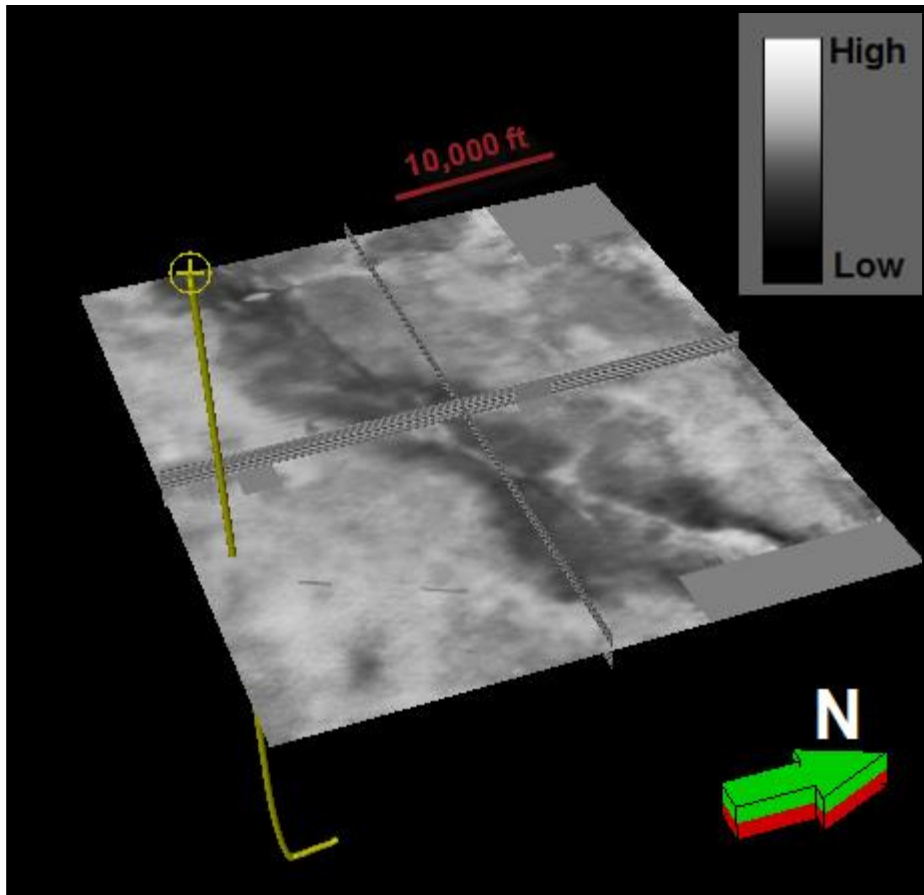


**Figure 10.** A cropped amplitude volume of the 3D seismic survey in the time domain. A single well displayed that is incorrectly lined up with the seismic.

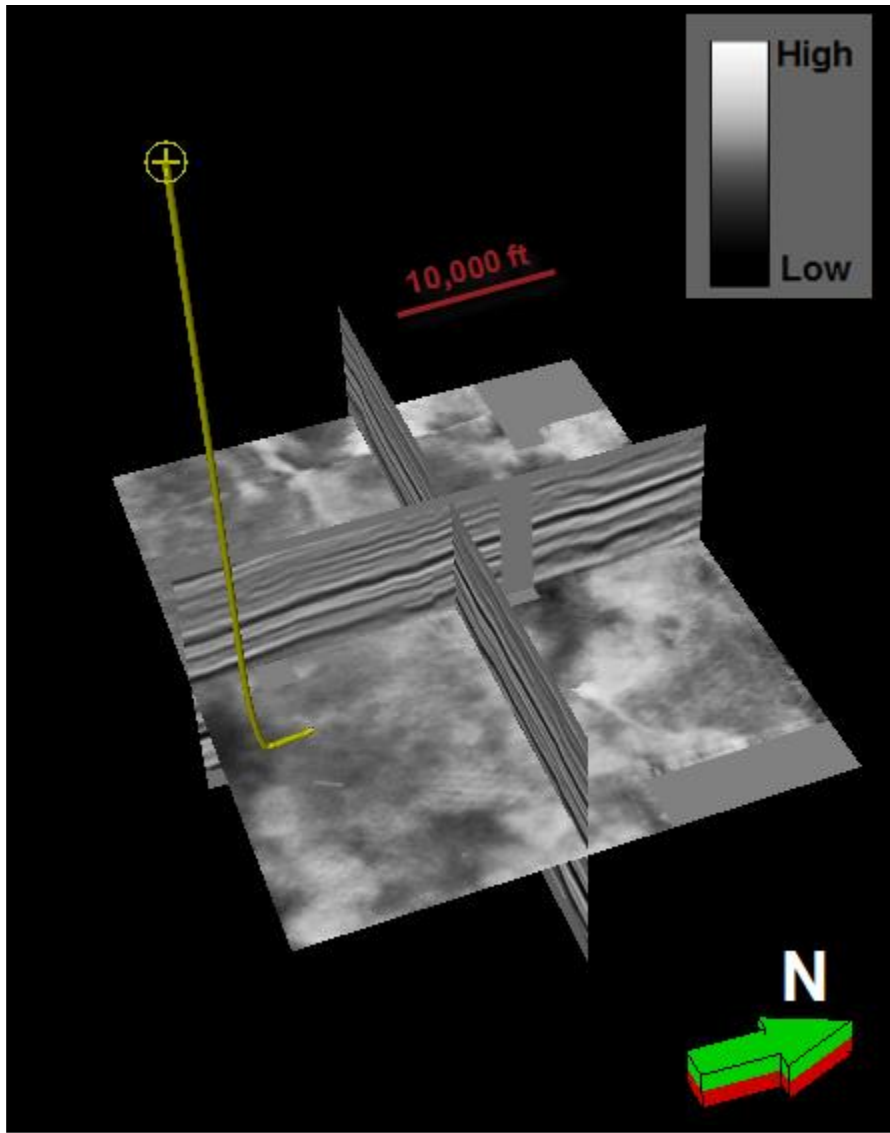


**Figure 11.** A cropped amplitude volume of the 3D seismic survey after being converted to the depth domain. A single well is displayed and it is now correctly lined up with the seismic.

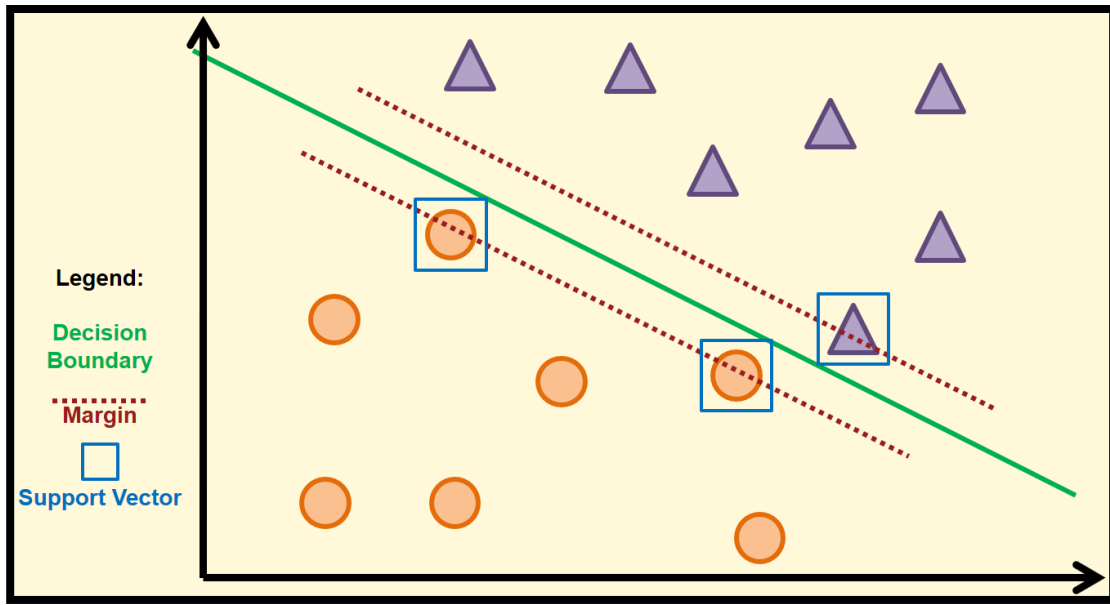


**Figure 12.** An example of a support vector machine in 2D space. The decision boundary, separating the two classes, is displayed by the solid green line. The margins are denoted by the dashed crimson line and the support vectors are highlighted by the blue boxes (After Cortes and Vapnik, 1995).

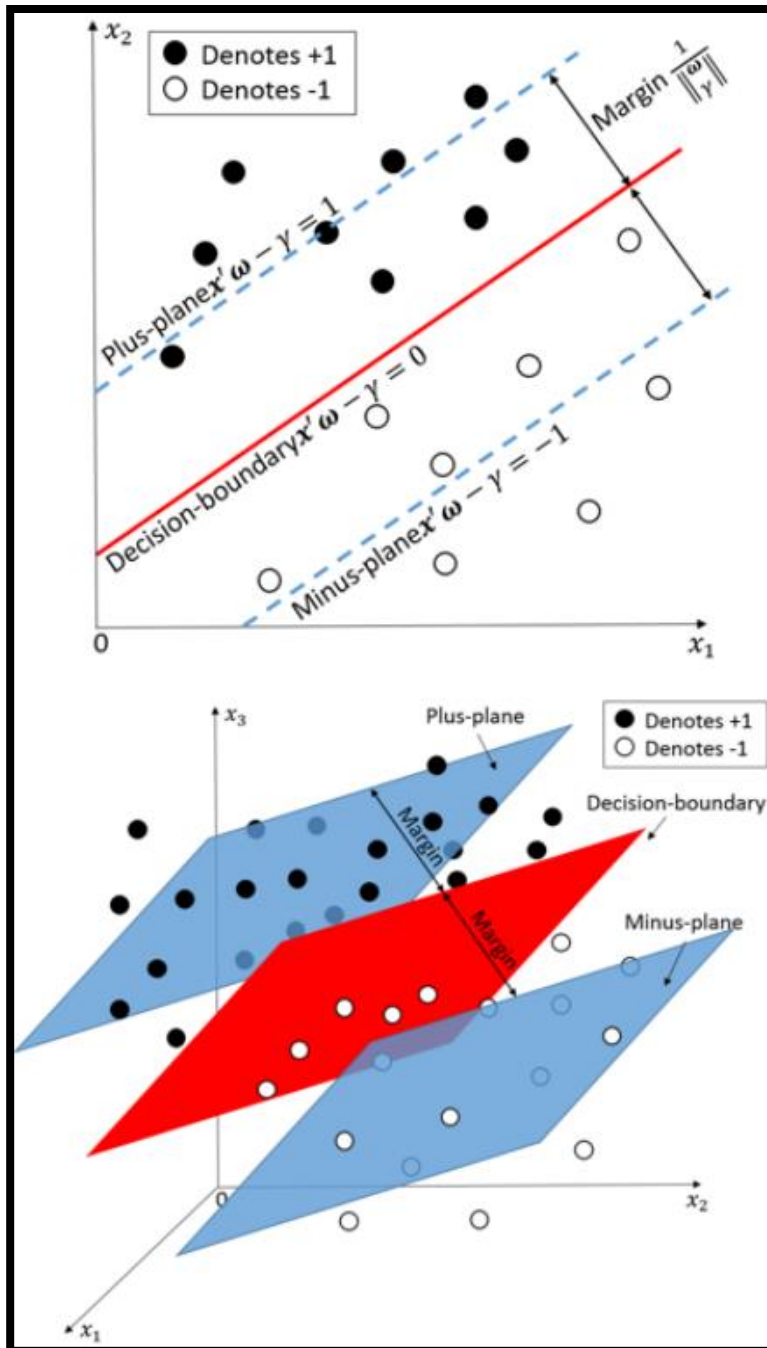


**Figure 13.** An example of a binary class PSVM. The upper graph is in 2D space and the decision boundary is defined by the red line. The lower picture shows a set of points in 3D space where the decision boundary is now defined by the red plane (Modified from Zhao et al. 2014).

```
C:\Windows\system32\cmd.exe
item[bar]=100
item[mpbar]=20
item[CUmaxloop]=10

[psvm_welllogs.exe]
[CUmaxloop=10]
[bar=100]
[c=2]
[delta=0.095]
[mode=1]
[mpbar=20]
[n=5]
[nonlinear_result_fn=psvm_welllogs_NorthAlva_Train+Test.txt]
[nskip=1]
[suffix=Train+Test]
[testing_fn=C:\Users\snyd9504\Desktop\PSUM_2_PointBased\Test.txt]
[training_fn=C:\Users\snyd9504\Desktop\PSUM_2_PointBased\Train.txt]
[unique_project_name=NorthAlva]
[v=2000]

Program is running in testing mode.
Data read finished.
Boundary No.      1 is generating...
Number of samples used for generating this boundary is      224
      0
      0 Matrix inverse finished
Matrix nu generated
before matmul
after matmul
Boundary No.      1 is generated successfully
Nonlinear PSUM finished
The number of correct classification using nonlinear PSUM is      25 out of
      40
The correlation coefficient using nonlinear PSUM is 0.2503130
Testing result has been saved to file:
psvm_welllogs_NorthAlva_Train+Test.txt

normal completetion. routine psvm_welllogs
```

**Figure 14.** A sample PSVM output. In this test, the model successfully classified 25 of the 40 testing points, or about 63%.

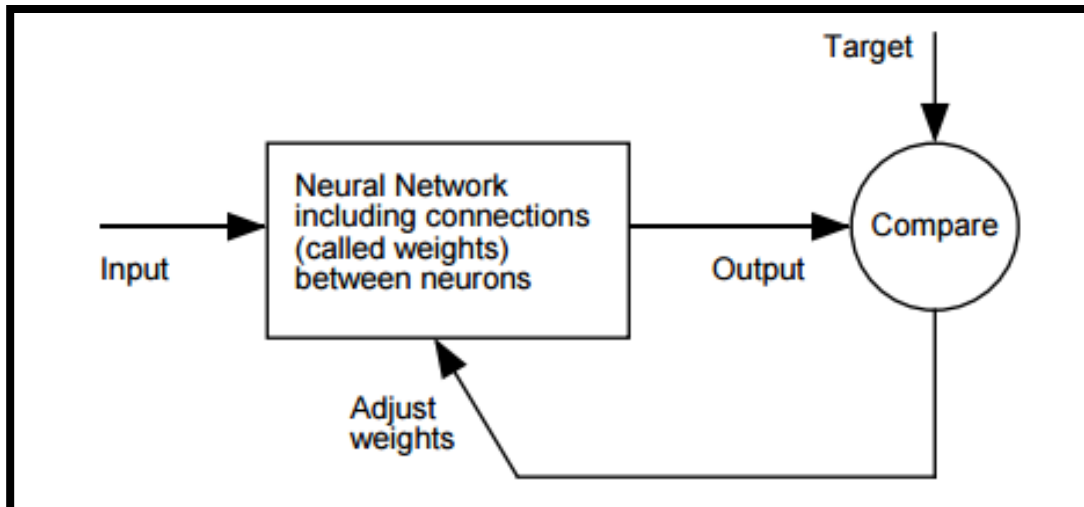


**Figure 15.** A generalized ANN workflow. Inputs are entered into the network where hidden neurons are defined and weights are given to each input variable. The output is compared to the targets and the neural network completes iterations until an optimal model is created (Demuth and Beale, 1993).

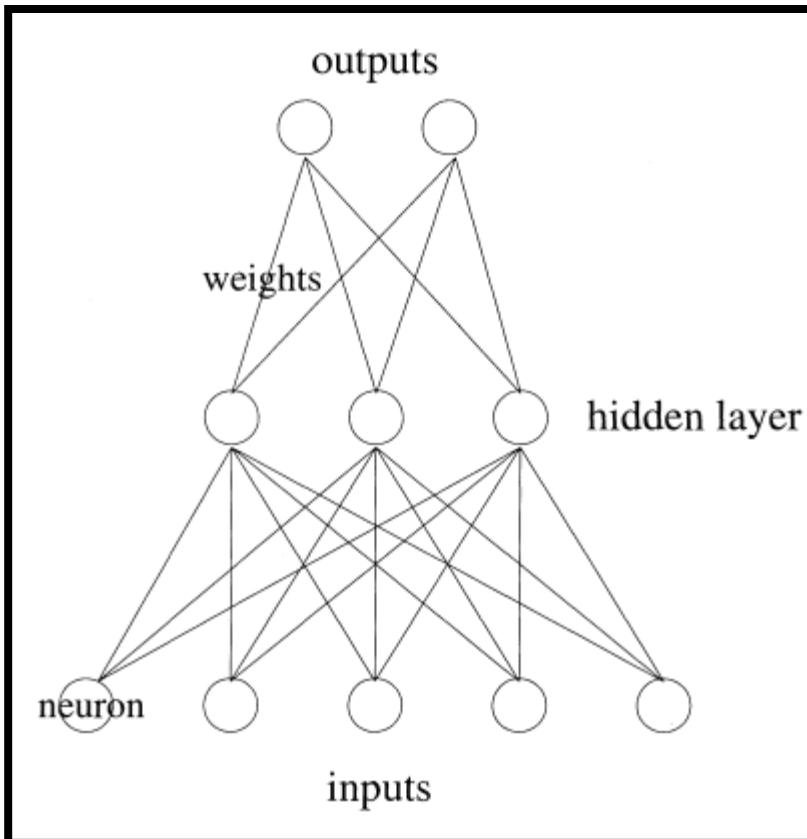
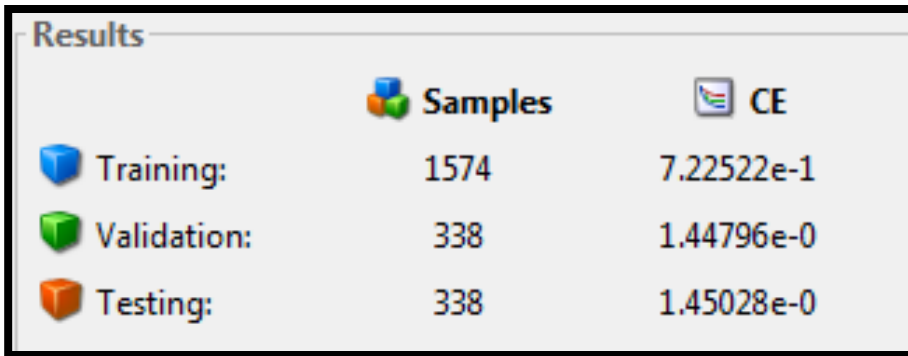


**Figure 16.** A of the structure of an ANN. It is characterized by inputs, neurons, a hidden layer, variable weights and outputs (Wang, 2003).



The image shows a screenshot of a MATLAB Results window. The window has a title bar that says "Results". Inside, there is a table with three columns: "Samples" (with a 3D cube icon), "CE" (with a document icon), and a third column for labels. The rows are "Training:", "Validation:", and "Testing:". The values for Samples are 1574, 338, and 338 respectively. The values for CE are 7.22522e-1, 1.44796e-0, and 1.45028e-0 respectively.

	Samples	CE
Training:	1574	7.22522e-1
Validation:	338	1.44796e-0
Testing:	338	1.45028e-0

**Figure 17.** An output from MATLAB’s Neural Pattern Recognition toolbox. “CE” stands for Cross-Entropy and values for this example are high meaning that this is a poor output model.

## Chapter 5: Exploratory Data Analysis

The data for the following results and analysis was sampled at every 110 ft. Cost of penetration is sampled at every two feet; however, the seismic was sampled every 110 ft. For this study, the COP data sample interval was upscaled to that of the seismic sample. Unlike ROP, the upscaled value of COP in (min/ft) is simply its arithmetic average (over 110 ft). Values of COP were estimated, through interpolation, at every 110 ft and corresponding values for geomechanical and geometric attributes were found at each sample point. This constitutes the data for this thesis.

### Visualization

The first step to understanding the data is through visualization. Figure 18 shows the entire raw and normalized COP histograms. Both histograms show that the COP is biased to the left, with about 66% of the total lateral length drilled faster than 1.82 min/ft and 37% drilled slower than 1.82 min/ft. This distribution will be used to determine the threshold COP (or discriminator) for each class.

Figure 19 shows boxplots of the input geomechanical and geometric attributes for this data set. The histograms are broken up into five classes based on their respective COP value at each point - Class 1 representing low COP and 5 representing high COP. At first glance, it is difficult to discern between classes as there appears to be a great amount of overlap among all five classes. In other words, there is not a clear decision boundary.

Figure 20 displays box plots for P-impedance, inverted porosity, curvedness,  $\lambda\rho$ , and  $\mu\rho$ . Two classes are displayed; Class 1 representing low COP while class 2

represents high COP. The classes are easier to distinguish in these figures; however, there still does not appear to be high amounts of separation within the data.

## **Proximal Support Vector Machine**

### *Five Classes*

The first set of data tested in the PSVM was the collection broken up into five classes. Figure 21 shows the results between the training and testing data. The PSVM correctly classified 67 of the 292 data points, or about 23%. The results of this test are disappointing. 77% of the time, the PSVM misclassified the points based on the input values. In an attempt to increase the correctness, the range of classes was decreased from 5 to 2.

### *Two Classes*

Figure 22 displays the results from a 2-class PSVM test on the entire data set. The model created correctly classified 154 of the 292 data points. About 53% of the times, the model will correctly classify points based on the input variables. While this is an increase of 30% from the 5-class model, it is still inadequate for the purpose of classification.

## **Artificial Neural Network**

### *Five Classes*

Figure 23 shows output confusion matrix from an artificial neural network that created a 5-class model. The model used 70%, 15% and 15% of the data for training, validation and testing, respectively. The confusion matrix shows that the ANN correctly classified the data points about 24% of the time. Figure 24 shows that the cross-entropy for this model is 0.78, 1.36 and 1.43 for the training, validation and testing data,

respectively; an ideal value for cross-entropy is 0 meaning no error. Following suit, a 2 class model was developed in an effort to increase the classification correctness.

### *Two Classes*

An ANN was used to create a 2 class COP model for the data. The model used 70%, 15% and 15% of the data for training, validation and testing, respectively. Figure 25 shows an output confusion matrix for this set of data. The model correctly classified about 66% of the tested data, but incorrectly placed almost every class 2 point. In addition, the cross-entropy shown in Figure 26 is about 0.45, 0.68 and 0.68 for the training, validation and testing data, respectively.

### **Discussion**

Overall, the results for the initial exploratory data analysis were unfortunately poor. Both 5-class models performed significantly worse than the 2-class models. This is most likely due to the inability for the PSVM and ANN to create a decision boundary between the classes of data. In other words, it is more difficult to cluster data split into 5 classes than it is to cluster data split into 2 classes. Another issue may be due to drilling techniques. If a well is drilled in a different manner, or with a separate set of standards than another well, the COP could vary accordingly making the classification technique more difficult.

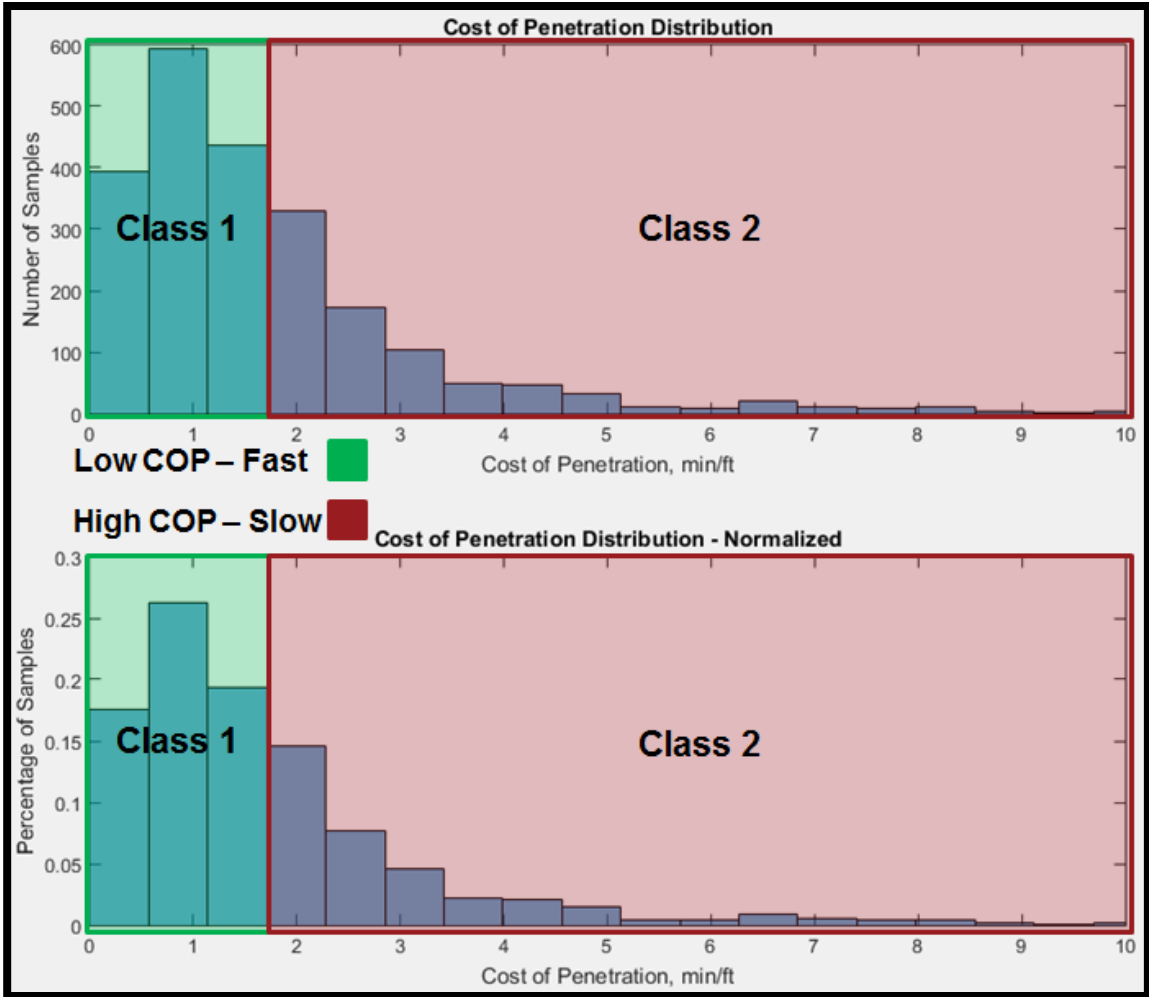


**Figure 18.** Two histograms showing the distribution (upper) and normalized distribution (lower) for cost of penetration. Both graphs are skewed right showing that the majority of the values of COP are on the lower end of the distribution.

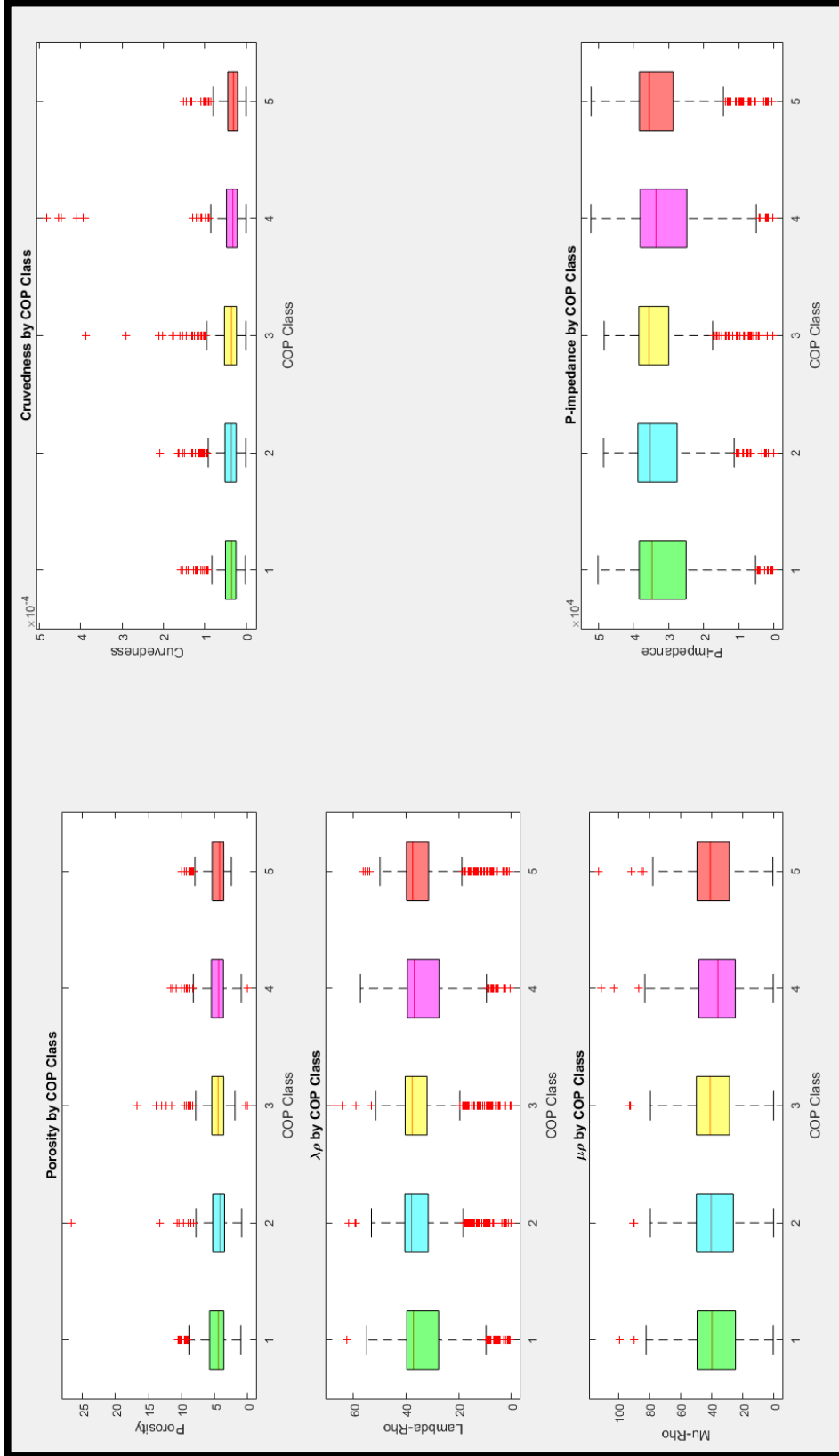


**Figure 19.** Five boxplots displaying five input parameters for this study. The points are broken into 5 classes. Class 1 being the lowest COP and Class 5 being the highest COP. There is no clear separation between the five classes.

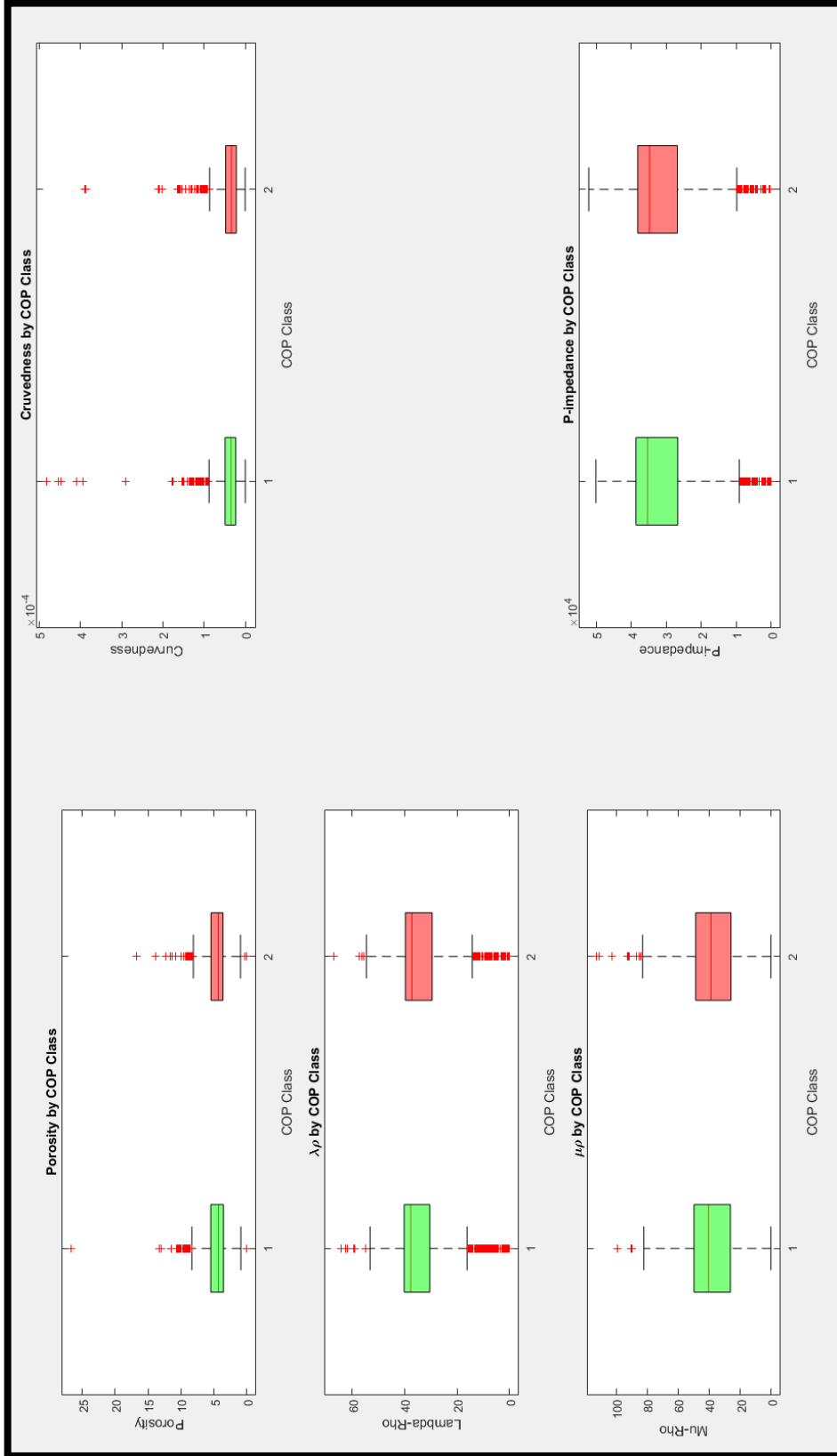


**Figure 20.** Five boxplots displaying the input parameters for this study. The points are broken into 2 classes. Class 1 being lower COP and Class 2 being higher COP. A visual discriminator is difficult to define.

```
C:\Windows\system32\cmd.exe
Boundary No.      6 is generated successfully
Boundary No.      7 is generating...
Number of samples used for generating this boundary is      519
      0
      0 Matrix inverse finished
Matrix nu generated
before matmul
after matmul
Boundary No.      7 is generated successfully
Boundary No.      8 is generating...
Number of samples used for generating this boundary is      567
      0
      0 Matrix inverse finished
Matrix nu generated
before matmul
after matmul
Boundary No.      8 is generated successfully
Boundary No.      9 is generating...
Number of samples used for generating this boundary is      508
      0
      0 Matrix inverse finished
Matrix nu generated
before matmul
after matmul
Boundary No.      9 is generated successfully
Boundary No.     10 is generating...
Number of samples used for generating this boundary is      518
      0
      0 Matrix inverse finished
Matrix nu generated
before matmul
after matmul
Boundary No.     10 is generated successfully
Nonlinear PSUM finished
The number of correct classification using nonlinear PSUM is      67 out of
      292
The correlation coefficient using nonlinear PSUM is -1.7227214E-02
Testing result has been saved to file:
psvm_wellogs_NorthAlva_Train+Test.txt

normal completetion. routine psvm_wellogs
```

**Figure 21.** Output for the 5-class PSVM. This model correctly classified 67 of the 292 testing points, or about 23%.

```
ca: C:\Windows\system32\cmd.exe
item[mpbar]=20
item[CUMaxloop]=1

[psvm_welllogs.exe]
[CUMaxloop=1]
[bar=30]
[c=2]
[delta=0.1]
[mode=1]
[mpbar=20]
[n=5]
[nonlinear_result_fn=psvm_welllogs_NorthAlva_Train+Test.txt]
[nskip=1]
[suffix=Train+Test]
[testing_fn=C:\Users\snyd9504\Desktop\Data Analysis_REDUX\PSUM_2\PSUM2_Test.txt]

[training_fn=C:\Users\snyd9504\Desktop\Data Analysis_REDUX\PSUM_2\PSUM2_Train.txt]
[unique_project_name=NorthAlva]
[v=2000]

Program is running in testing mode.
Data read finished.
Boundary No.      1 is generating...
Number of samples used for generating this boundary is      576
      0
      0 Matrix inverse finished
Matrix nu generated
before matmul
after matmul
Boundary No.      1 is generated successfully
Nonlinear PSUM finished
The number of correct classification using nonlinear PSUM is      154 out of
      292
The correlation coefficient using nonlinear PSUM is  7.2135732E-02
Testing result has been saved to file:
psvm_welllogs_NorthAlva_Train+Test.txt

normal completion. routine psvm_welllogs
```

**Figure 22.** Output for the 2-class PSVM. This model correctly classified 154 of the 292 testing points, or about 53%.

**All Confusion Matrix**

Output Class	1	193 8.6%	141 6.3%	158 7.0%	190 8.4%	141 6.3%	23.5% 76.5%
	2	124 5.5%	186 8.3%	135 6.0%	127 5.6%	139 6.2%	26.2% 73.8%
	3	0 0.0%	1 0.0%	2 0.1%	0 0.0%	0 0.0%	66.7% 33.3%
	4	141 6.3%	132 5.9%	131 5.8%	159 7.1%	141 6.3%	22.6% 77.4%
	5	1 0.0%	2 0.1%	2 0.1%	2 0.1%	2 0.1%	22.2% 77.8%
			42.0% 58.0%	40.3% 59.7%	0.5% 99.5%	33.3% 66.7%	0.5% 99.5%
		1	2	3	4	5	
		<b>Target Class</b>					

**Figure 23.** Confusion matrix for the 5-class ANN. This model correctly classified about 24% of the testing points.

Results		
	 Samples	 CE
 Training:	1462	7.77167e-1
 Validation:	450	1.36451e-0
 Testing:	338	1.43030e-0

**Figure 24.** Output results for the 5-class ANN. The cross-entropy for the training, validation and testing data is about 0.78, 1.36 and 1.43, respectively.

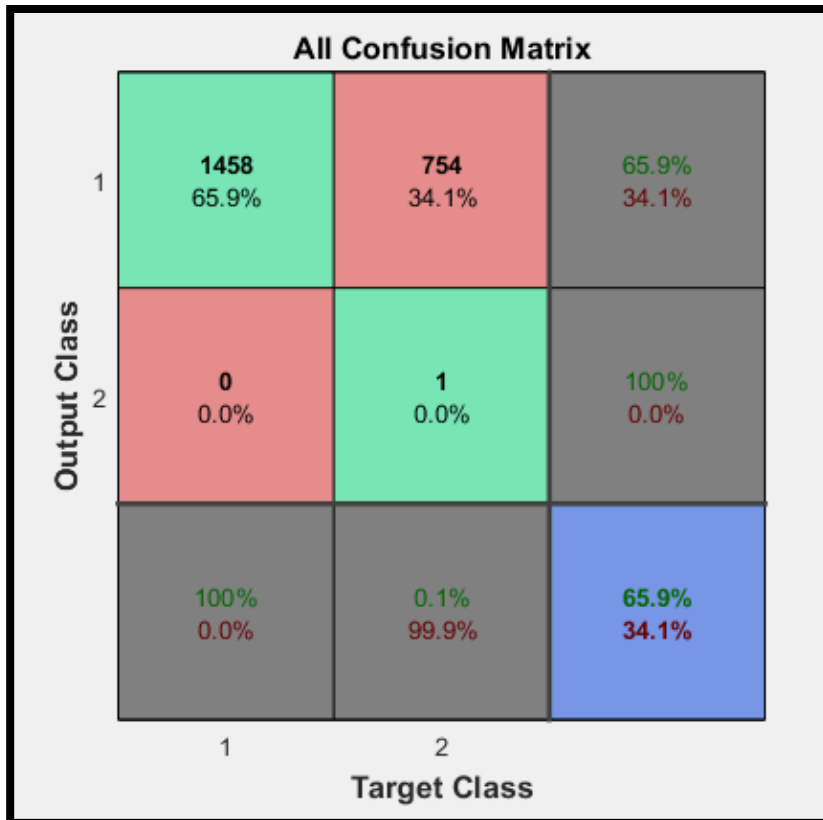


**Figure 25.** Confusion matrix for the 2-class ANN. This model correctly classified about 66% of the testing points.

Results		
	 Samples	 CE
 Training:	1549	4.48406e-1
 Validation:	332	6.83312e-1
 Testing:	332	6.82476e-1

**Figure 26.** Output results for the 2-class ANN. The cross-entropy for the training, validation and testing is 0.45, 0.68 and 0.68, respectively.

## Chapter 6: Directional Driller Analysis

One variable not used in the previous chapter was that of the directional drilling company. Many oil and gas service companies contract out directional drillers to drill the lateral segments of wells. Different companies may have different drilling practices, or the drillers they employ may have differing amounts of experience than other drillers in the area. That being said, COP rates may vary greatly between directional drilling services. When time is of the essence, and time is money, the most efficient directional drilling service is a sought-after asset.

This chapter seeks to remove the directional drilling factor by looking at three individual sets of wells drilled by three different directional drillers. By doing so, wells that were drilled in similar fashion will be compared with each other. Previously, the conglomerate of wells compared had been drilled by many different companies and, most likely, with different drilling practices. In multivariate statistical analysis, the drilling company is another attribute that needs to be addressed. Classes will be defined by mean COP. By doing this, we can visualize the percentage of time – or cost – that is spent drilling Class 1 and Class 2 portions of a drillers lateral wellbore.

### Directional Driller 1

#### *Visualization*

Directional Driller 1 drilled five laterals in the study area (Figure 27). The distribution for COP and normalized COP can be seen in Figure 28. Combining this with Table 2, Directional Driller 1 can be better characterized. We can see that Directional Driller 1 spent 50% of the time drilling on 27% of the lateral segments of the five wells. This driller had a mean COP of 0.99 min/ft and a median of 0.63 min/ft.

The standard deviation was about 0.96 min/ft. The COP is skewed right with a skewness of 3.47. Hypothetically, Directional Driller 1 would be able to drill a 5000 ft lateral in 3.44 days.

Two classes, high and low COP, were defined by the mean COP value for each set of wells. Figure 29 displays five input boxplots for Directional Driller 1. Visual decision boundaries are more evident than in the previous chapter for the data points. This should yield an increase in correctness.

#### *Proximal Support Vector Machine*

Figure 30 displays the output from the PSVM for Directional Driller 1. The input variables are P-impedance, inversion porosity, curvedness,  $\lambda\rho$  and  $\mu\rho$ . The PSVM correctly placed 34 of the 40 testing points into the correct class. This corresponds to a correctness of about 85%. This is a significant increase from the previous models generated with the PSVM.

#### *Artificial Neural Network*

Figure 31 shows the output confusion matrix of an ANN created for Driller 1. The model correctly classified 73% of the data, but misclassified every class 2 point. The cross-entropy for the training, validation and testing data was 0.46, 0.73 and 0.75, respectively, as shown by Figure 32. This shows a correctness increase from the previous ANN; however, the cross-entropy values for the validation and testing samples increases.

## **Directional Driller 2**

### *Visualization*

Five laterals were drilled by Directional Driller 2 in the study area (Figure 33). Figure 34 displays the distribution and normalized distribution of COP for these wells. Table 3 displays a statistical breakdown for the COP. We can see that Directional Driller 2 spent 50% of the time drilling on 36% of the lateral segments of the five wells. Directional Driller 2 had a mean COP of 1.16 min/ft, a median of 0.98 min/ft and a standard deviation of 0.80 min/ft. Theoretically, Directional Driller 2 would drill a 5000 ft lateral in approximately 4.03 days.

Figure 35 shows five boxplots for the input geomechanical and geometric attributes for this driller. As with Directional Driller 1, decision boundaries have become clearer – the data is more easily separated.

### *Proximal Support Vector Machine*

The results of the 2-class PSVM for Directional Driller 2 are shown in Figure 36. Of the 40 testing points, the PSVM correctly classified 28, or about 70%. The PSVM correctness for Directional Driller 2 is lower than the correctness for Directional Driller 1. Again, this is an increase from the PSVM model created using the entire set of data.

### *Artificial Neural Network*

The confusion matrix displayed in Figure 37 shows that the model created by the ANN correctly classified 64% of the data, but misclassified every class 2 point. Figure 38 shows that the cross-entropy for the training, validation and testing data was 0.45, 0.69 and 0.69, respectively. The correctness values are lower than those of

Directional Driller 1. This model has a decrease in correctness from the ANN model created using the whole data set, but the cross-entropy values remain about the same.

### **Directional Driller 3**

#### *Visualization*

Directional Driller 3 drilled the lateral portion of seven wells in this study area (Figure 39). Figure 40 shows the distribution of COP as well as the normalized distribution of COP. We can see that Directional Driller 3 spent 50% of the time drilling on 32% of the lateral segments of the seven wells. Statistical parameters for the COP of this driller are displayed in Table 4. Directional Driller 3 has a mean, median and standard deviation COP of 2.91 min/ft, 2.03 min/ft and 2.77 min/ft, respectively. This Direction Driller could drill a 5000 ft lateral in about 10.1 days.

Figure 41 displays five boxplots for the input attributes from these seven wells. Similar to the input histograms for Directional Driller 1 and Directional Driller 2, it is discriminators between the two classes are easier to visualize.

#### *Proximal Support Vector Machine*

Figure 42 shows the results from the 2-class PSVM for Directional Driller 3. The PSVM correctly classified 28 of the 40 testing points or about 70%. The correctness is similar to Directional Driller 2 and an increase from the PSVM created for the entire data set.

#### *Artificial Neural Network*

Figure 43 displays the confusion matrix from an ANN for Directional Driller 3; the network makes correct classifications about 66% of the time; however, the model misclassified almost every class 2 point. The cross-entropy displayed in Figure 44

shows that the values for the training, validation and testing data is 0.45, 0.69 and 0.69, respectively. These values are comparable to Directional Driller 2 mentioned previously, but this is not improvement from the 2-class ANN created for the entire data set.

### **Discussion**

With the hypothesis that different drilling companies follow different drilling protocols and safety procedures that effect weight on bit and other parameters, I conducted a simple statistical analysis as well as PSVM and ANN prediction of COP for the three directional drilling companies. By separating the drillers and using a 2-class PSVM and ANN, I found that the classification correctness increased from the 2-class PSVM and ANN used to classify COP in the previous chapter.

Statistically, the COP varied between the three directional drillers. Direction Drillers 1, 2 and 3 had mean COP of 0.99, 1.16, and 2.91 min/ft, respectively. Median values of COP for these drillers are 0.63, 0.98 and 2.03 min/ft, respectively. Standard deviation of COP was 0.96, 0.80 and 2.77 min/ft, respectively. The variability in mean, median and standard deviation of COP between the 3 drillers supports the idea that there are differing variable affecting the speed of the drillers and therefore the directional drillers should be evaluated separately.

When using the PSVM as a classification tool, the correctness for Directional Drillers 1, 2 and 3 is about 85%, 70% and 70%, respectively. This is an increase of 32%, 17% and 17% for Directional Driller 1, 2 and 3, respectively from the PSVM classification for the entire data set. The increase in correctness was significant.

Results were not as strong when using the ANN. The ANN generated for Directional Drillers 1, 2 and 3 classified points with correctness of about 73%, 64% and 66%, respectively. The correctness from the 2-class ANN used on the entire data set increased for driller 1, decreased for driller 2, and remained constant for driller 3. The increase in correctness was not as significant as the increase with PSVM. The results using the ANN lead me to believe that the PSVM is a stronger tool for classification.

By separately analyzing the three directional drillers, correctness for the PSVM increased; however, in some instances, the correctness of the ANN decreased. Previously, the data was analyzed without factoring in the directional driller. Accounting for the directional driller in the analysis helps to remove differences in drilling practices which, in turn, may affect the overall COP. This leads to – in four of the six cases – more correct classification results as can be seen in the previous discussion.

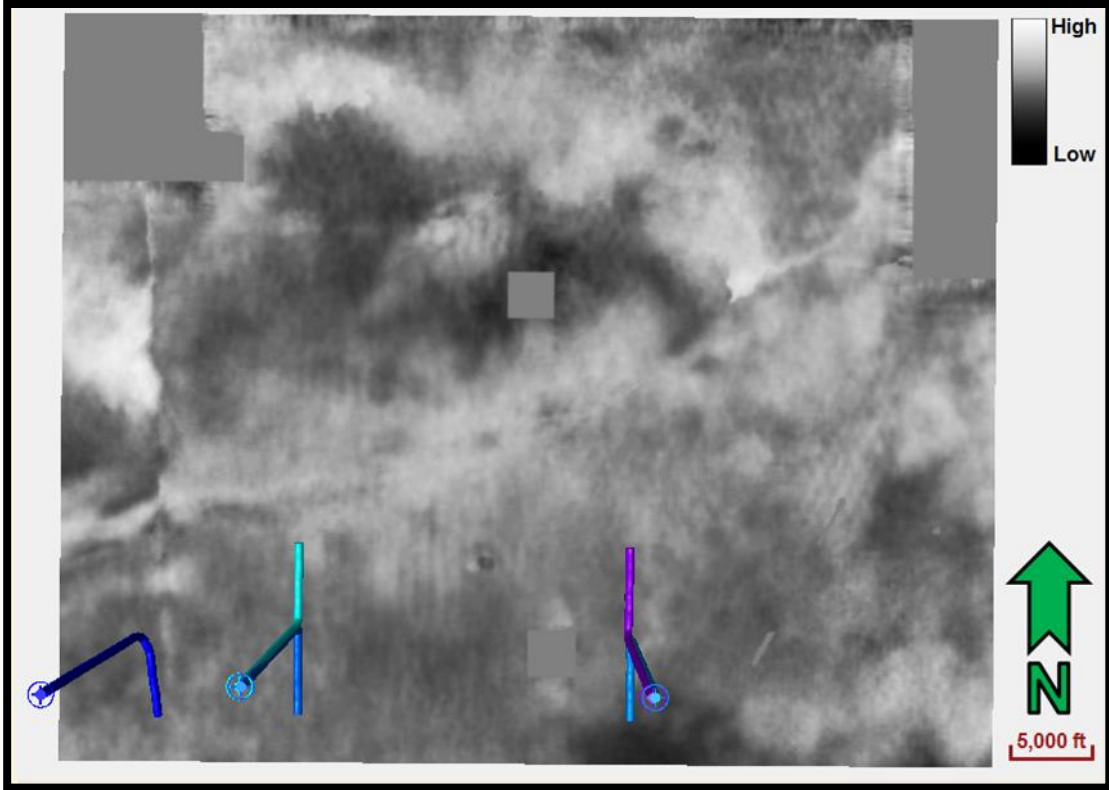


**Figure 27.** Cropped amplitude slice showing the location of Directional Driller 1's five lateral wells.

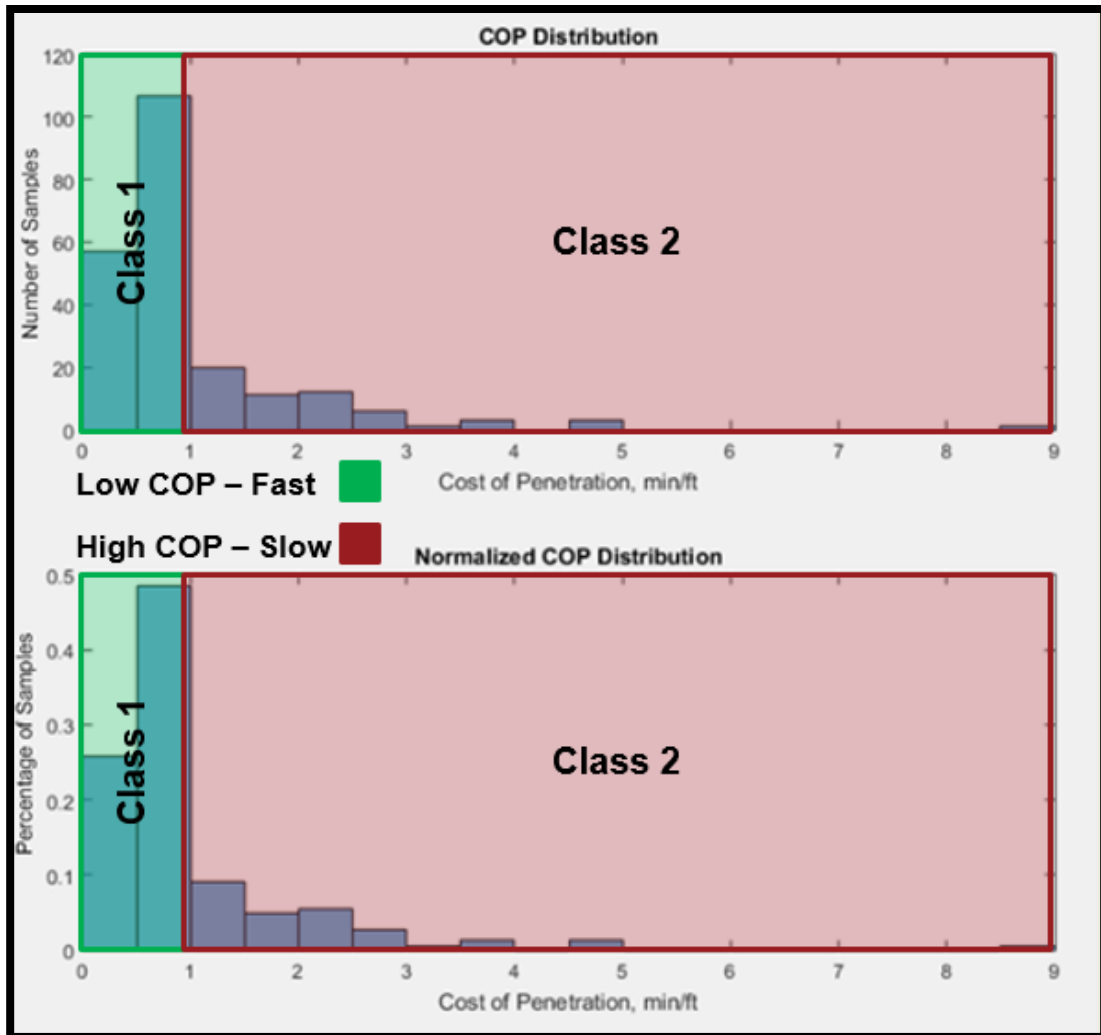


**Figure 28.** Two histograms showing the distribution (upper) and normalized distribution (lower) for cost of penetration for Directional Driller 1. Both graphs are skewed right showing that the majority of the values of COP are on the lower end of the distribution.

Directional Driller 1	
<b>Center:</b>	
Mean	0.99
Median	0.63
Mode	0.47
<b>Spread:</b>	
Range	8.67
Variance	0.92
Standard Deviation	0.96
<b>Shape:</b>	
Skewness	3.47
Kurtosis	18.46

**Table 2.** Basic statistics for cost of penetration of Directional Driller 1. Values to better characterize the center, spread and shape of the distribution are shown.

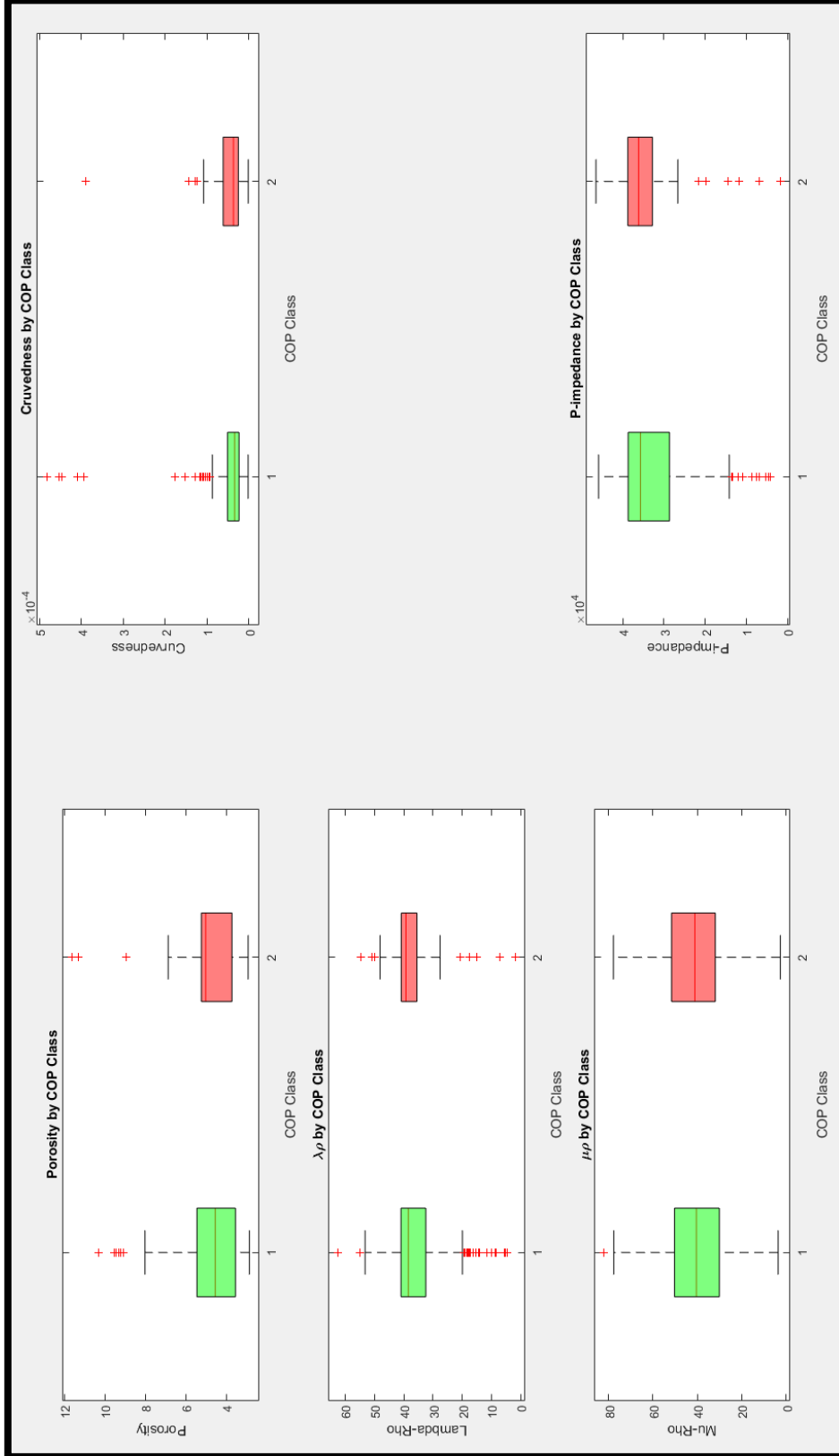


**Figure 29.** Five boxplots displaying the five input parameters for Directional Driller 1 in this study. The points are broken into 2 classes, Class 1 being low COP and Class 2 being high COP. There is more separation between the 2 classes than in the previous chapter.

```
C:\Windows\system32\cmd.exe
Program is running in testing mode.
Data read finished.
Boundary No.      1 is generating...
Number of samples used for generating this boundary is      226
0
0 Matrix inverse finished
Matrix nu generated
before matmul
after matmul
Boundary No.      1 is generated successfully
Nonlinear PSUM finished
The number of correct classification using nonlinear PSUM is      34 out of
40
The correlation coefficient using nonlinear PSUM is -6.0522757E-02
Testing result has been saved to file:
psvm_welllogs_N0_I+I.txt

normal completion. routine psvm_welllogs
```

**Figure 30.** Output for the 2-class PSVM for Directional Driller 1. This model correctly classified 34 of the 40 testing points, or about 85%.

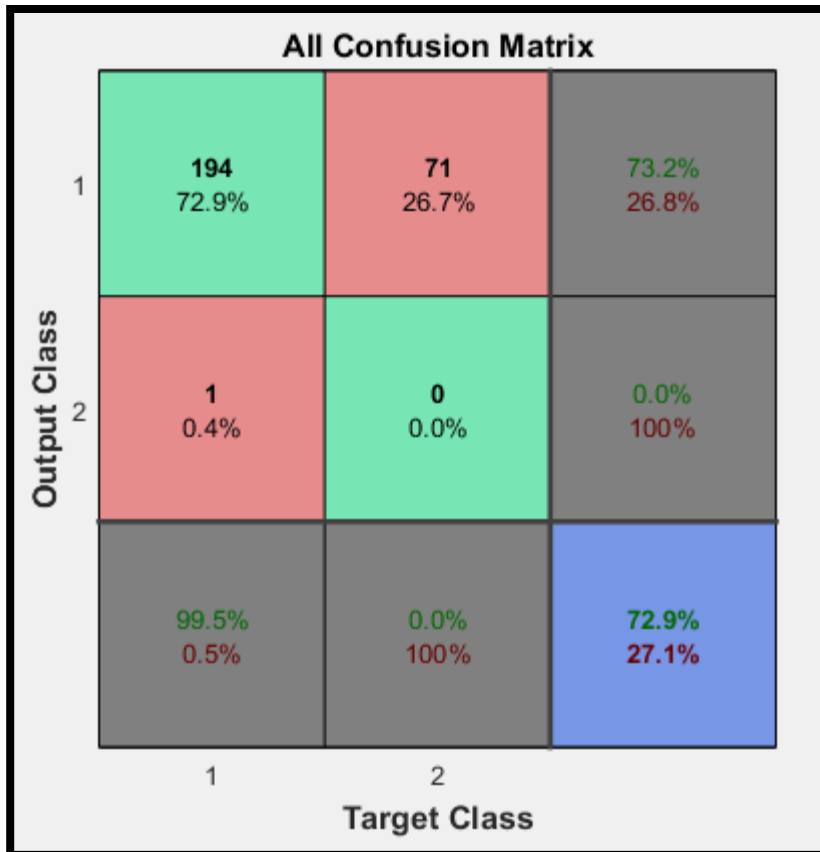


**Figure 31.** Confusion matrix for the 2-class ANN for Directional Driller 1. This model correctly classified about 73% of the testing points.

The image shows a window titled "Results" with a table of performance metrics. The table has three columns: a label (Training, Validation, Testing), "Samples", and "CE" (Cross-Entropy). The data is as follows:

	Samples	CE
Training:	186	4.58126e-1
Validation:	40	7.32113e-1
Testing:	40	7.45507e-1

**Figure 32.** Output results for the 2-class ANN for Directional Driller 1. The cross-entropy for the training, validation and testing data is about 0.46, 0.73 and 0.75, respectively.

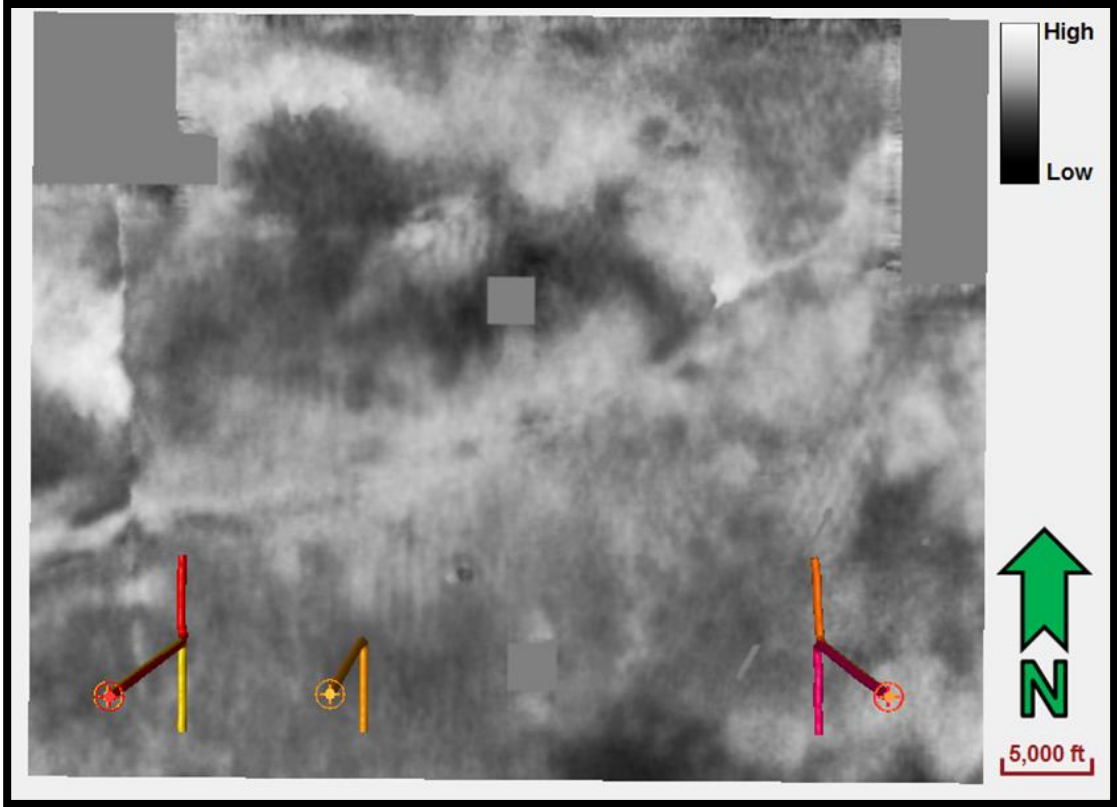


**Figure 33.** Cropped amplitude slice showing the location of Directional Driller 2's five lateral wells.

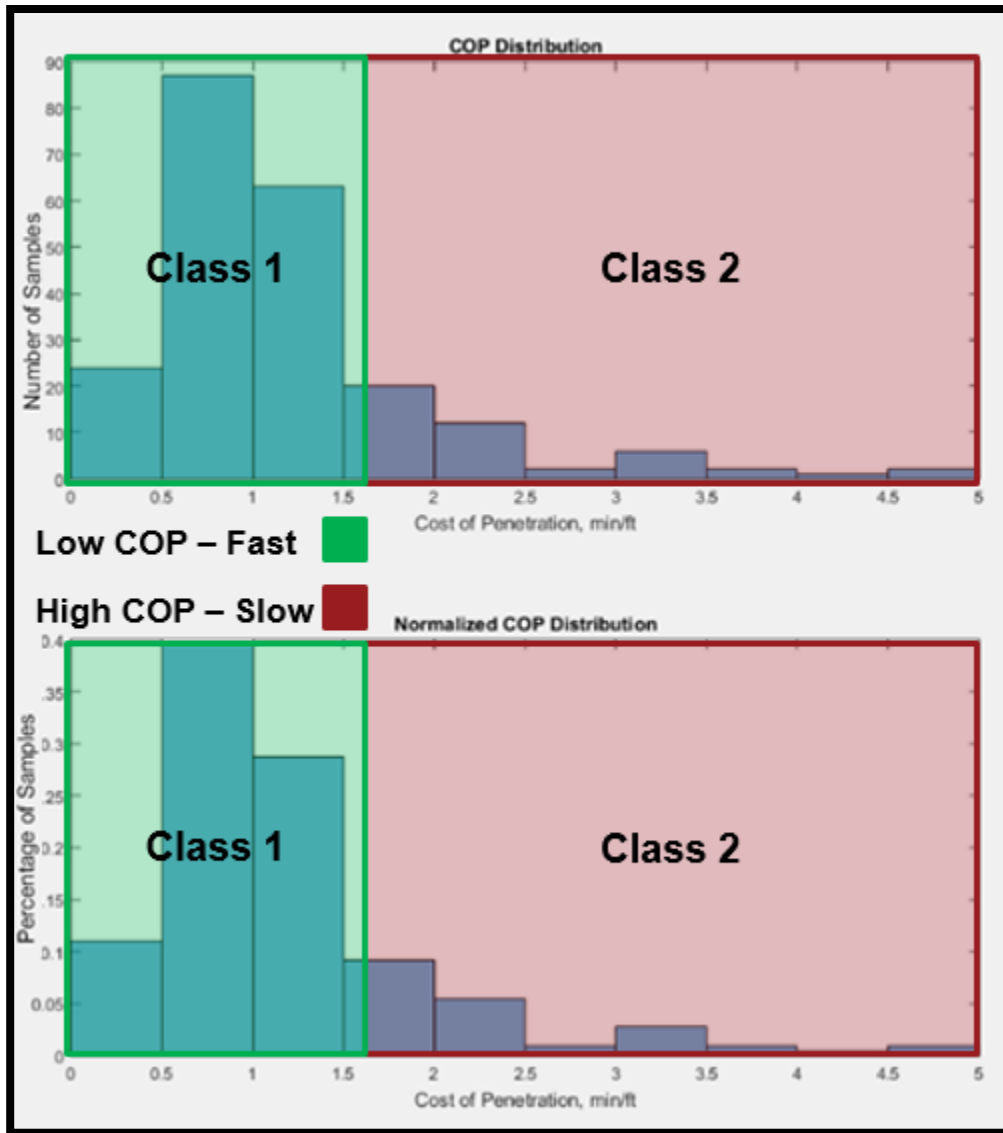


**Figure 34.** Two histograms showing the distribution (upper) and normalized distribution (lower) for cost of penetration for Directional Driller 2. Both graphs are skewed right showing that the majority of the values of COP are on the lower end of the distribution.

Directional Driller 2	
<b>Center:</b>	
Mean	1.16
Median	0.98
Mode	0.68
<b>Spread:</b>	
Range	4.83
Variance	0.64
Standard Deviation	0.80
<b>Shape:</b>	
Skewness	2.25
Kurtosis	6.47

**Table 3.** Basic statistics for cost of penetration of Directional Driller 2. Values to better characterize the center, spread and shape of the distribution are shown.

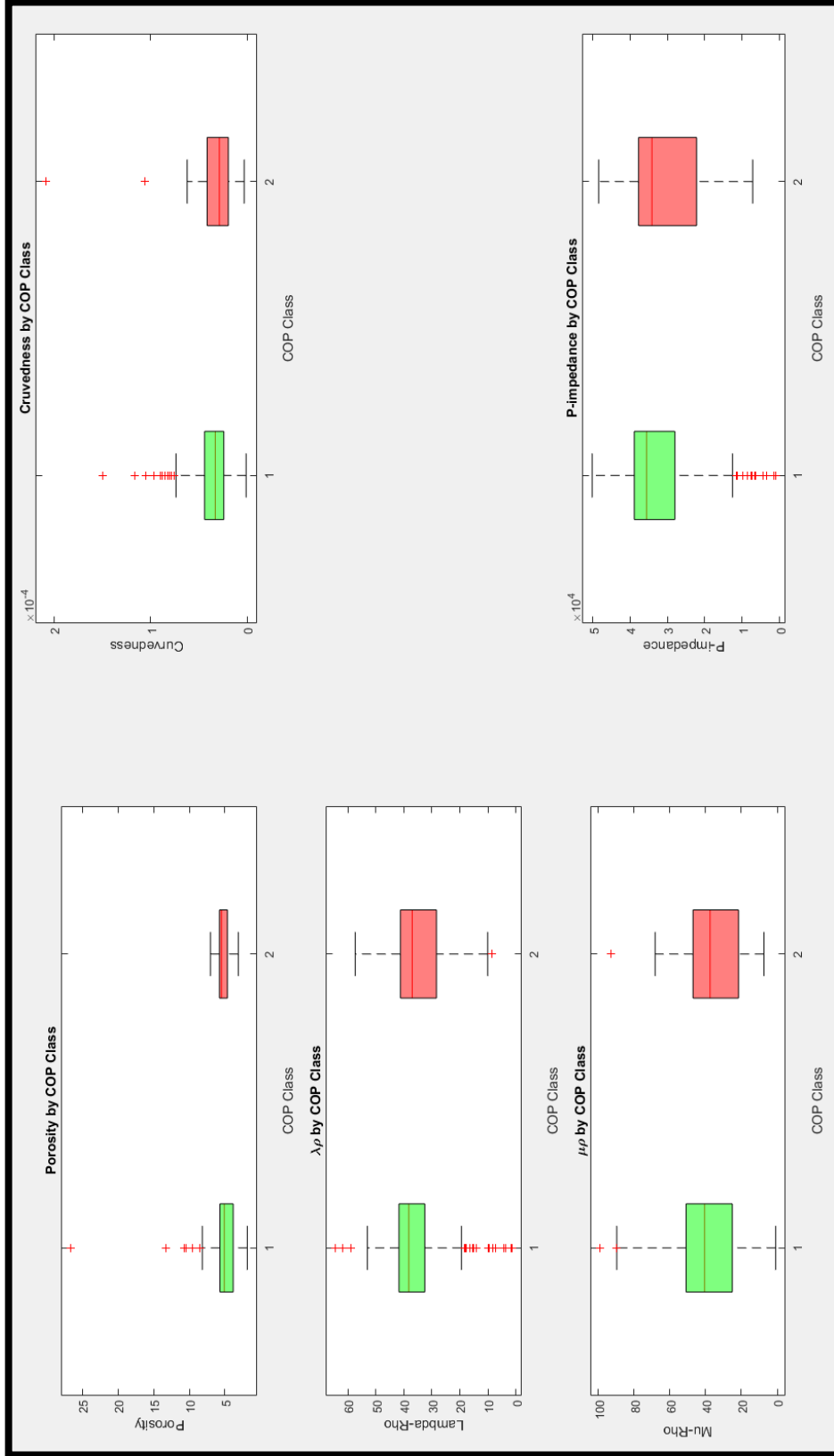


**Figure 35.** Five boxplots displaying the five input parameters for Directional Driller 2 in this study. The points are broken into 2 classes. Class 1 being low COP and Class 2 being high COP. There is more separation between the 2 classes than in the previous chapter.

```
CAWindows\system32\cmd.exe
Program is running in testing mode.
Data read finished.
Boundary No.      1 is generating...
Number of samples used for generating this boundary is      224
0
0 Matrix inverse finished
Matrix nu generated
before matmul
after matmul
Boundary No.      1 is generated successfully
Nonlinear PSUM finished
The number of correct classification using nonlinear PSUM is      28 out of
40
The correlation coefficient using nonlinear PSUM is 0.2882784
Testing result has been saved to file:
psvm_wellogs_N0_1+I.txt

normal completion. routine psvm_wellogs
```

**Figure 36.** Output for the 2-class PSVM for Directional Driller 2. This model correctly classified 28 of the 40 testing points, or about 70%.

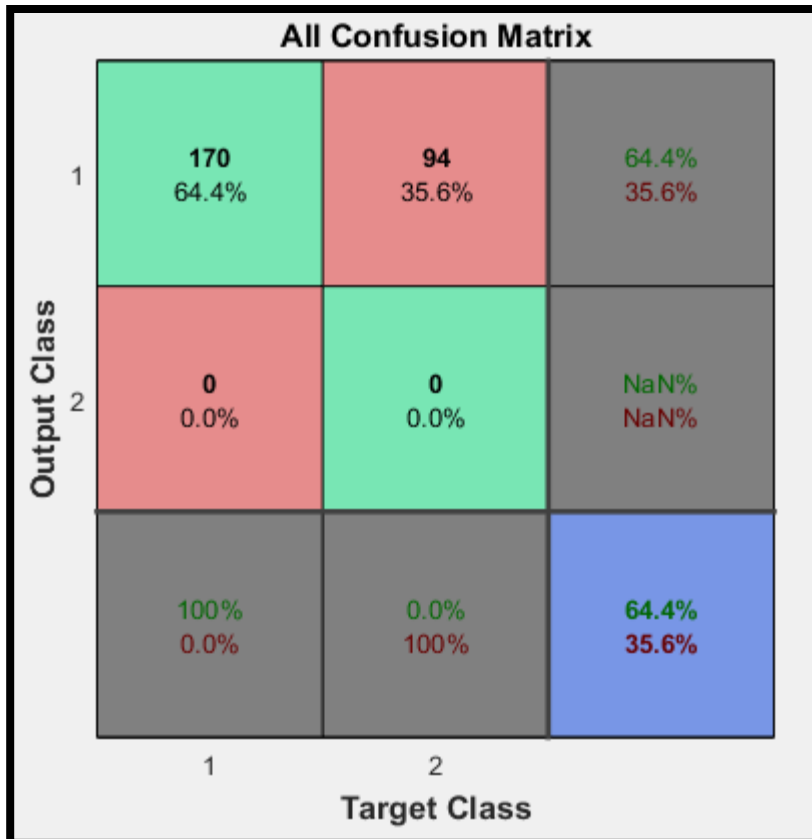


**Figure 37.** Confusion matrix for the 2-class ANN for Directional Driller 2. This model correctly classified about 64% of the testing points.

Results		
	 Samples	 CE
 Training:	184	4.49469e-1
 Validation:	40	6.87515e-1
 Testing:	40	6.92588e-1

**Figure 38.** Output results for the 2-class ANN for Directional Driller 2. The cross-entropy for the training, validation and testing data is about 0.45, 0.69 and 0.69, respectively.

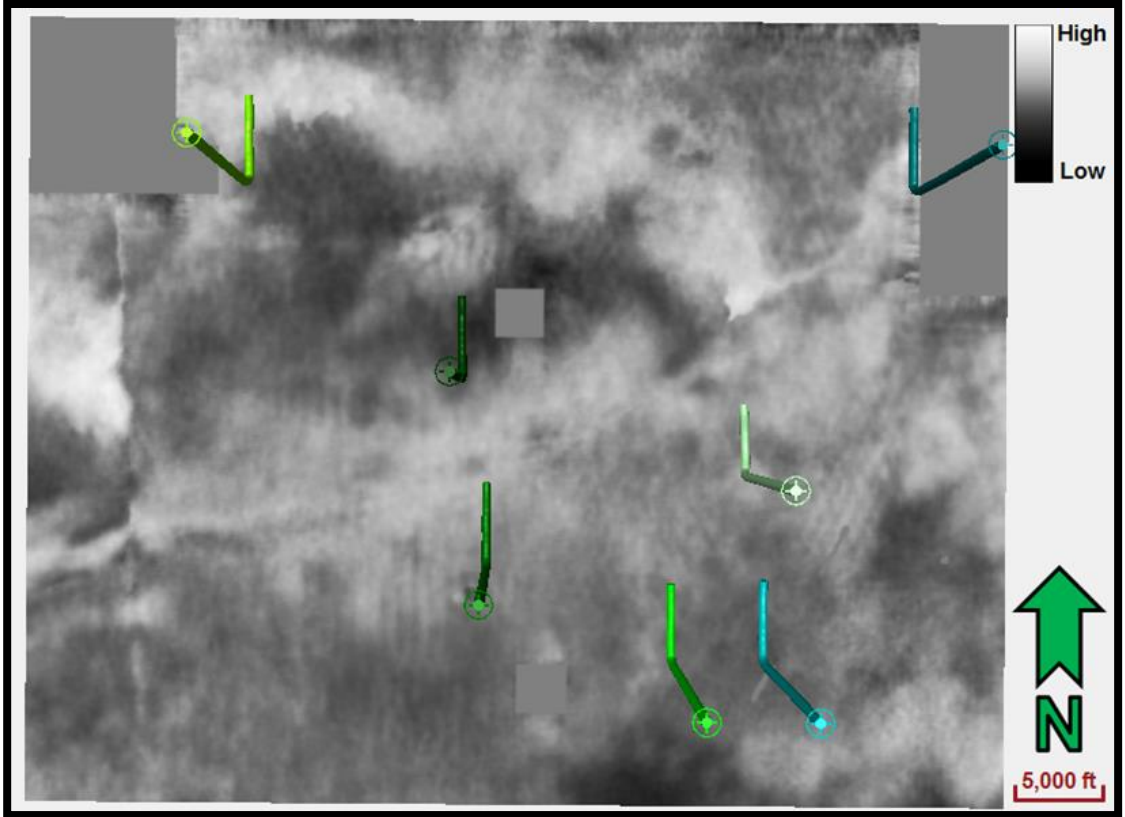


**Figure 39.** Cropped amplitude slice showing the location of Directional Driller 3's seven lateral wells.

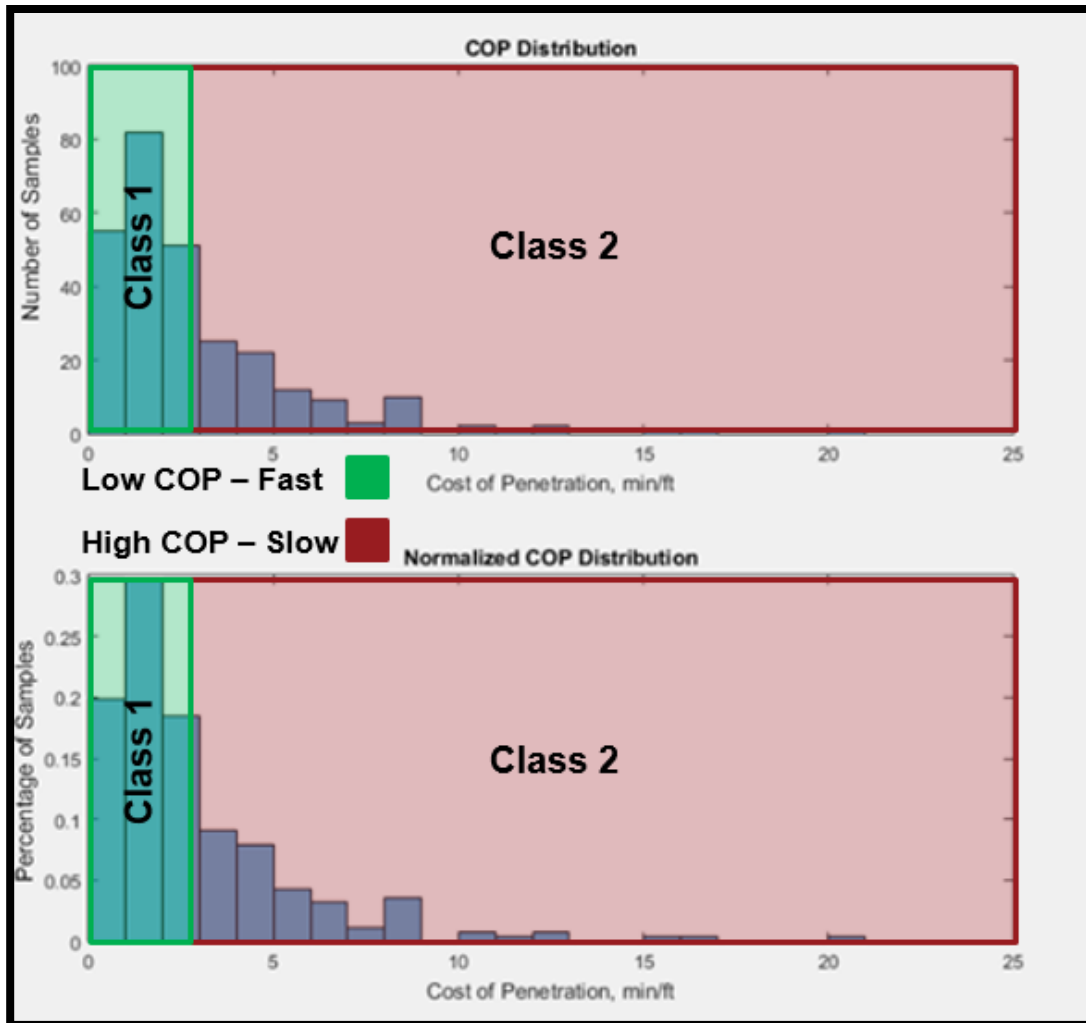


**Figure 40.** Two histograms showing the distribution (upper) and normalized distribution (lower) for cost of penetration for Directional Driller 3. Both graphs are skewed right showing that the majority of the values of COP are on the lower end of the distribution.

Directional Driller 3	
<b>Center:</b>	
Mean	2.91
Median	2.03
Mode	0.45
<b>Spread:</b>	
Range	20.53
Variance	7.67
Standard Deviation	2.77
<b>Shape:</b>	
Skewness	2.61
Kurtosis	9.81

**Table 4.** Basic statistics for cost of penetration of Directional Driller 3. Values to better characterize the center, spread and shape of the distribution are shown.

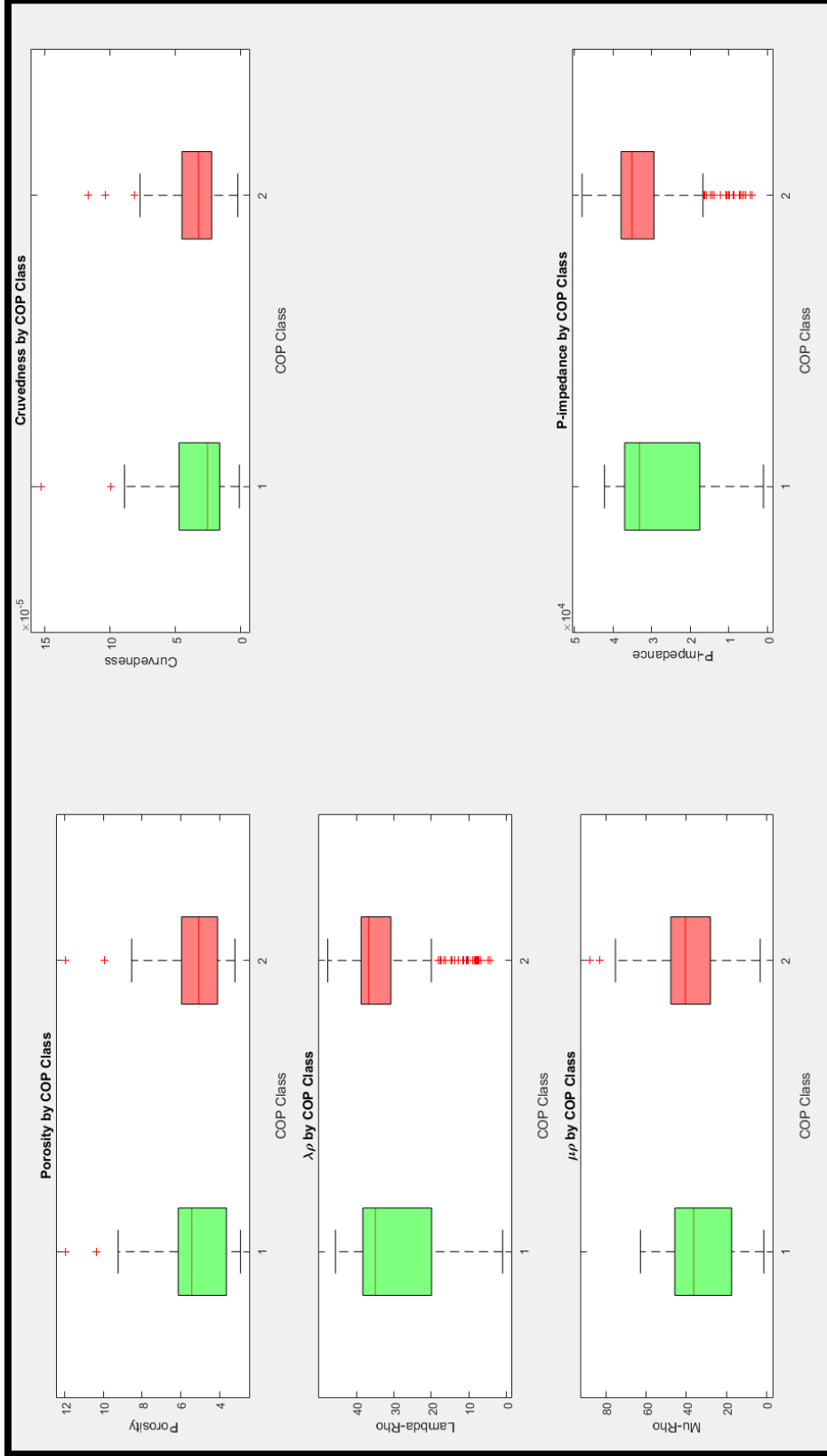


**Figure 41.** Five boxplots displaying the five input parameters for Directional Driller 3 in this study. The points are broken into 2 classes. Class 1 being low COP and Class 2 being high COP. There is more separation between the 2 classes than in the previous chapter.

```
ca. C:\Windows\system32\cmd.exe
Program is running in testing mode.
Data read finished.
Boundary No.      1 is generating...
Number of samples used for generating this boundary is      237
0
0 Matrix inverse finished
Matrix nu generated
before matmul
after matmul
Boundary No.      1 is generated successfully
Nonlinear PSUM finished
The number of correct classification using nonlinear PSUM is      28 out of
40
The correlation coefficient using nonlinear PSUM is 0.1058097
Testing result has been saved to file:
psvm_wellogs_NA_Test+Train.txt

normal completion. routine psvm_wellogs
```

**Figure 42.** Output for the 2-class PSVM for Directional Driller 3. This model correctly classified 28 of the 40 testing points, or about 70%.

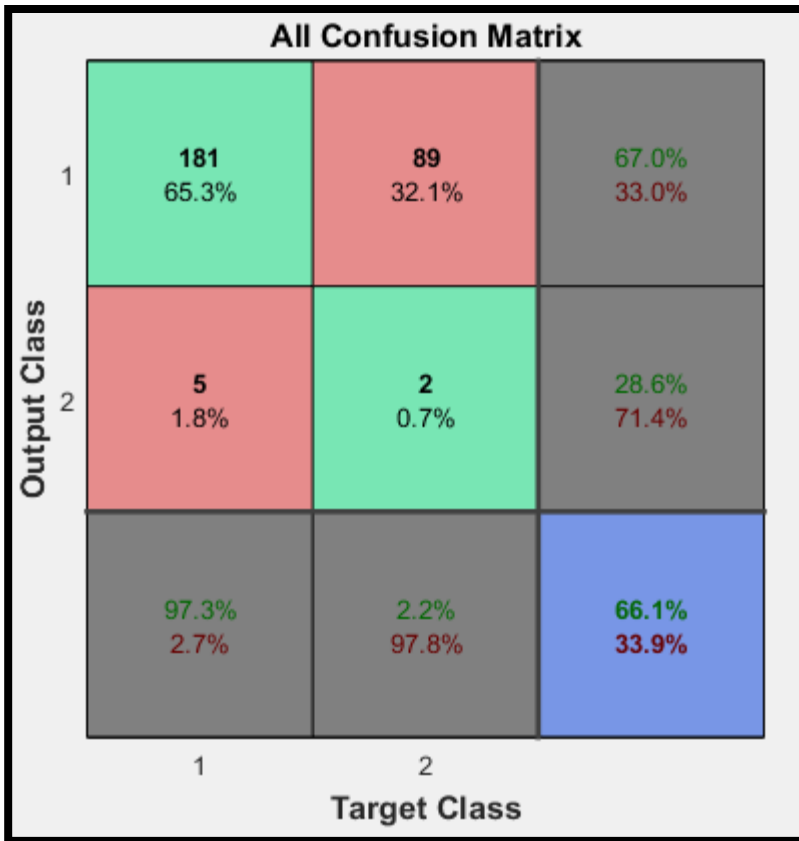


**Figure 43.** Confusion matrix for the 2-class ANN for Directional Driller 3. This model correctly classified about 66% of the testing points.

Results		
	 Samples	 CE
 Training:	193	4.48911e-1
 Validation:	42	6.89990e-1
 Testing:	42	6.89788e-1

**Figure 44.** Output results for the 2-class ANN for Directional Driller 3. The cross-entropy for the training, validation and testing data is about 0.45, 0.69 and 0.69, respectively.

## Chapter 7: Bit Trip Analysis

Tripping in and out of the borehole to replace a drill bit is a costly process when drilling a well. Bourgoyne et al. (1986) outlined the drilling cost equation as

$$C_f = \frac{C_b + C_r(t_b + t_c + t_t)}{\Delta D}, \quad (7)$$

where  $C_f$  is the drilled cost per unit foot,  $C_b$  is the cost of drill bits,  $C_r$  is the fixed operating cost,  $t_b$  is the rotating time,  $t_c$  is the nonrotating time,  $t_t$  is the trip time and  $\Delta D$  is the change in measured depth. When a bit breaks or fails and the operator must trip out of the borehole the trip time,  $t_t$ , increases and, with that, so does the overall cost. As an operator, minimizing the number of bit failures and bit trips can help to decrease drilling costs.

This chapter seeks to quantify bit trips in the lateral for two sets of horizontal wells drilled by two different directional drillers. As with the previous chapter, this seeks to minimize the amount of human error and differences between directional drillers. Class 1 is defined as 2-5 bit trips in the lateral and Class 2 is defined as 6-9 bit trips in the lateral (Figure 45). Using these two classes, Directional Driller 1 and Directional Driller 3 from the previous chapter are analyzed using a PSVM with inputs of eight GLCM texture attributes. One well was removed from the analysis on Directional Driller 3 as I believe the reported data on bit trips may be incorrect. Directional Driller 2 was removed from this Chapter as all of their wells fell within Class 1.

## **Directional Driller 1**

### *Visualization*

Two classes were defined for bit trips. Figure 46 shows the distribution of the eight input GLCM texture attributes by bit class. The input variables are GLCM contrast, correlation, dissimilarity, energy, entropy, homogeneity, mean and variance. Visually, differences in these input values can be made for Class 1 and Class 2 points from the boxplots. This allows for easier discrimination between the two classes.

### *Proximal Support Vector Machine*

Figure 47 shows the results from the 2-class PSVM for Directional Driller 1. The PSVM correctly classified 37 of the 40 testing points or about 93%. This is a very strong correctness factor which means the accuracy for a bit trip model would be quite high.

## **Directional Driller 3**

### *Visualization*

Figure 48 displays eight input boxplots for Directional Driller 3. Visual decision boundaries are evident between the two classes. As with Directional Driller 1, this should be indicative of higher PSVM correctness results.

### *Proximal Support Vector Machine*

Figure 49 displays the output from the PSVM for Directional Driller 3. The PSVM correctly placed 36 of the 40 testing points into the correct class. This corresponds to a correctness of about 90%. As with Directional Driller 1, these are strong results.

## Discussion

Through the use of a PSVM, I was able to correlate the number of bit trips in the lateral to GLCM texture attributes. By separating the drillers and using a 2-class PSVM, I found that the classification correctness to be 93% for Directional Driller 1 and 90% for Directional Driller 3. As with the previous chapter, I believe that the results would have been significantly weaker had I carried out this analysis on the data set as a whole. By successfully correlating these eight attributes with number of bit trips, an operator could better predict the number of bit trips and bits a specific driller would use when drilling a specific area.

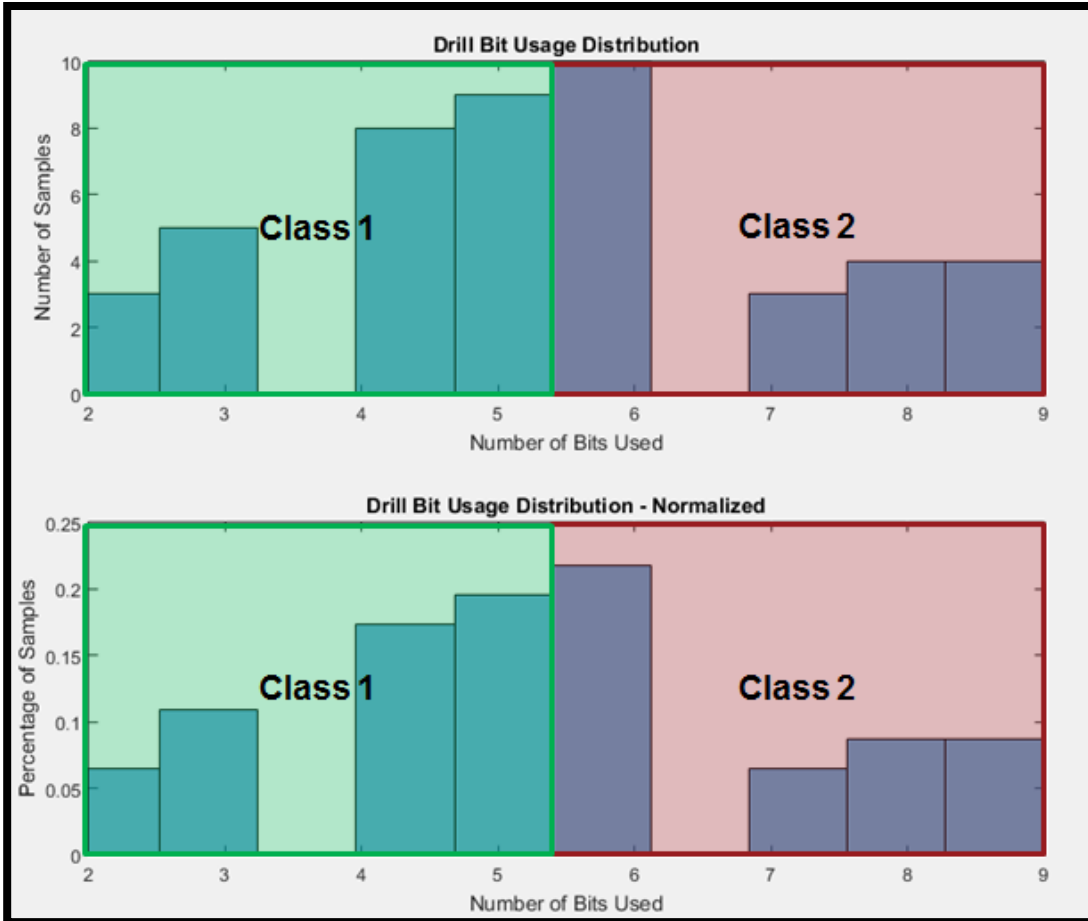


**Figure 45.** Two histograms showing the distribution (upper) and normalized distribution (lower) of bit trips for the 50 horizontal wells in the survey. Class 1 corresponds to wells that had 2-5 bit trips in the lateral, while Class 2 corresponds to wells that had 6-9 bit trips in the lateral.

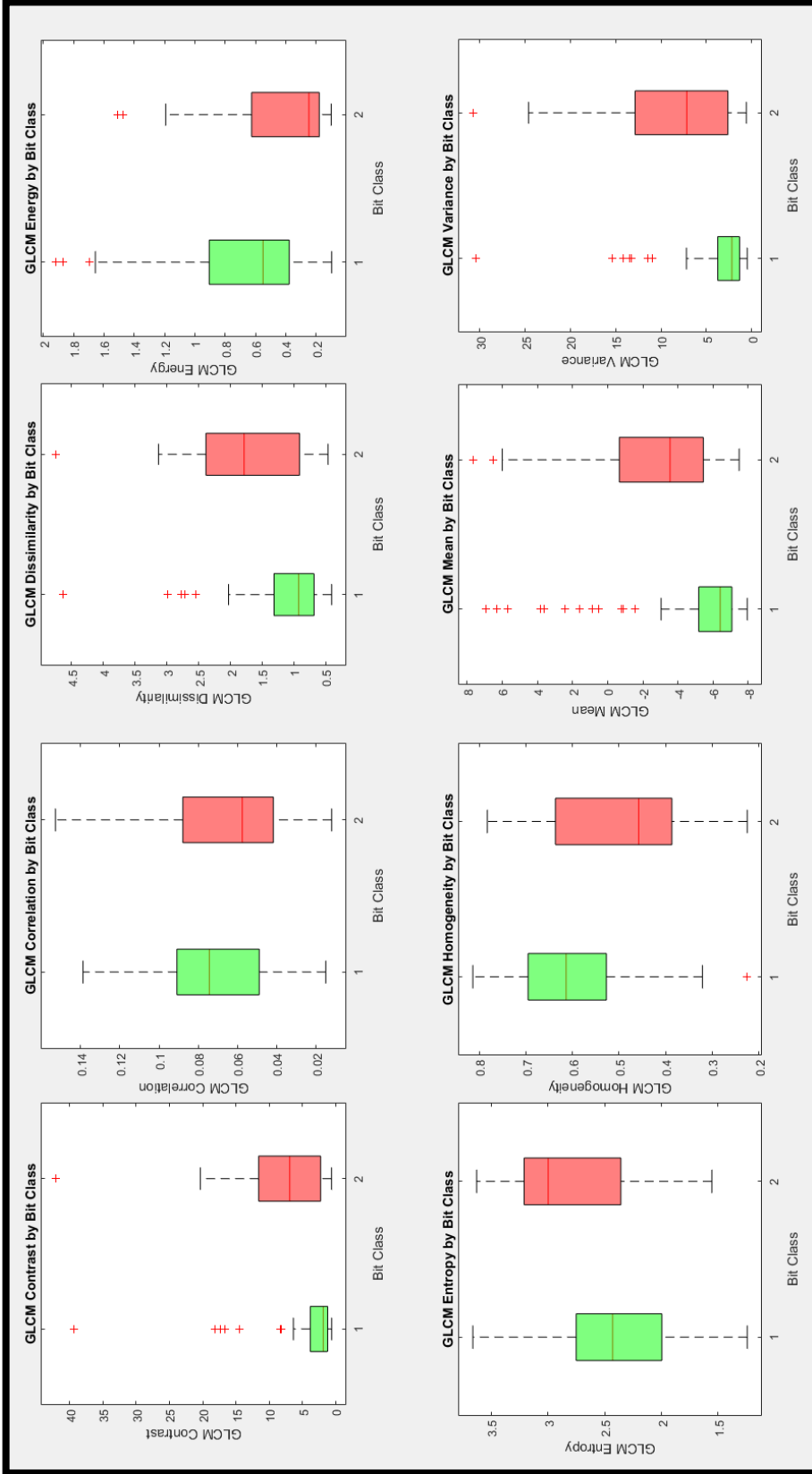


**Figure 46.** Eight boxplots displaying the eight input parameters for Directional Driller 1 in this chapter. The points are broken into 2 classes. Class 1 being 2-5 bit trips and Class 2 being 6-9 bit trips. Visual discriminators are easily understood.

```
C:\Windows\system32\cmd.exe

[psvm_wellogs.exe]
[Cumaxloop=1]
[bar=100]
[c=2]
[delta=0.1]
[mode=1]
[mpbar=20]
[n=8]
[nonlinear_result_fn=psvm_wellogs_NAGLCM_DD1.txt]
[nskip=1]
[suffix=DD1]
[testing_fn=C:\Users\snyd9504\Desktop\Drill Bits\DD1\test.txt]
[training_fn=C:\Users\snyd9504\Desktop\Drill Bits\DD1\train.txt]
[unique_project_name=NAGLCM]
[lv=2000]

Program is running in testing mode.
Data read finished.
Boundary No.          1 is generating...
Number of samples used for generating this boundary is          228
0
0 Matrix inverse finished
Matrix nu generated
before matmul
after matmul
Boundary No.          1 is generated successfully
Nonlinear PSUM finished
The number of correct classification using nonlinear PSUM is          37 out of
40
The correlation coefficient using nonlinear PSUM is 0.8432742
Testing result has been saved to file:
psvm_wellogs_NAGLCM_DD1.txt

normal completion. routine psvm_wellogs
```

**Figure 47.** Output for the 2-class PSVM for Directional Driller 1. This model correctly classified 37 of the 40 testing points, or about 93%.

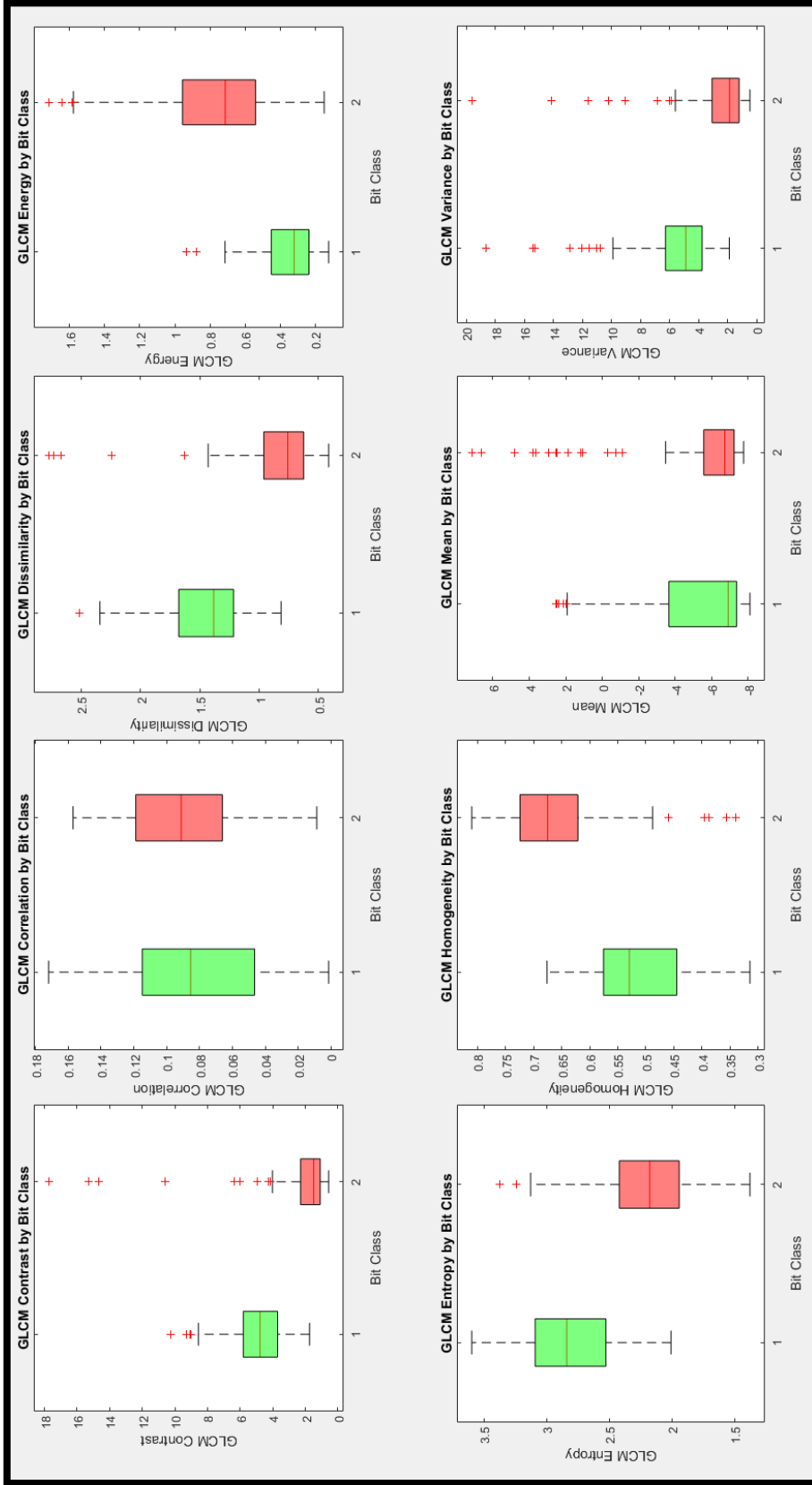


**Figure 48.** Eight boxplots displaying the eight input parameters for Directional Driller 3 in this chapter. The points are broken into 2 classes. Class 1 being 2-5 bit trips and Class 2 being 6-9 bit trips. Visual discriminators are easily understood.

```
C:\Windows\system32\cmd.exe
[psvm_wellogs.exe]
[CUmaxloop=1]
[bar=100]
[c=2]
[delta=0.4]
[mode=1]
[mpbar=20]
[n=8]
[nonlinear_result_fn=psvm_wellogs_NAGLCM_DD3.txt]
[nskip=1]
[suffix=DD3]
[testing_fn=C:\Users\snyd9504\Desktop\Drill Bits\DD3\test.txt]
[training_fn=C:\Users\snyd9504\Desktop\Drill Bits\DD3\train.txt]
[unique_project_name=NAGLCM]
[v=2000]

Program is running in testing mode.
Data read finished.
Boundary No.      1 is generating...
Number of samples used for generating this boundary is      219
      0
      0 Matrix inverse finished
Matrix nu generated
before matmul
after matmul
Boundary No.      1 is generated successfully
Nonlinear PSUM finished
The number of correct classification using nonlinear PSUM is      36 out of
      40
The correlation coefficient using nonlinear PSUM is 0.8164966
Testing result has been saved to file:
psvm_wellogs_NAGLCM_DD3.txt

normal completion. routine psvm_wellogs
```

**Figure 49.** Output for the 2-class PSVM for Directional Driller 3. This model correctly classified 36 of the 40 testing points, or about 90%.

## **Chapter 8: Conclusions**

Using a Proximal Support Vector Machine to predict cost of penetration has the potential to improve drilling practices not only in this study area, but in other fields as well. I believe that further research into this subject could yield stellar results. By removing the factor of the directional driller, I was able to increase the correctness by about 17-32% for a 2-class PSVM, but the 2-class ANN was not as strong. Through further analysis of drilling practices and input geomechanical and geometric attributes, this correctness would likely increase.

A Proximal Support Vector Machine is also a strong tool for predicting the number of bit trips in a lateral. When the factor of the directional driller was removed, I was able to achieve correctness of 90-93% for a 2-class PSVM. Similar to the COP analysis, I believe that additional investigation into other drilling parameters could yield stronger models with more classes.

I believe that this workflow can be used to statistically predict drilling costs for an operator who is established in a specific area. PSVM predictions, based on geomechanical and geometric attributes and updated with mudlog data from new wells, can provide the operator with statistical data to better estimate drilling costs. An operator, coupling these data with estimates of TOC and completion success, could better plan their drilling schedule and location of wells.

### **Recommendations for Future Work**

I believe that further study into this subject could produce strong results and change the way wells are planned and drilled in the future. I suggest that the following things ideas be evaluated:

1. Capture directional driller and service company name in addition to rig name to better classify COP and bit trips,
2. Explore factors such as drill bit design, drilling fluid and pump operation,
3. Evaluate correlation with 3D lithologic geocellular models,
4. Correlate bit wear to lithologic facies, and
5. Correlate fracture density from image logs to COP and bit trips.

## References

- Blakey, R., 2014, North American key time-slice paleogeographic maps, <http://cpgeosystems.com/namkeyframe.html>, Accessed March 22, 2016.
- Bourgoyne Jr., A. T., M. E. Chenevert, K. K. Millheim, and F. S. Young Jr., 1986, Applied drilling engineering: Society of Petroleum Engineers.
- Bowles Jr, J. P. F., 1961, Subsurface Geology of Woods County, Oklahoma: Oklahoma City Geological Society, Shale Shaker Digest, **3**, 197-215.
- Chopra, S., and K. J. Marfurt, 2007, Seismic attributes for prospect identification and reservoir characterization: Society of Exploration Geophysicists.
- Cortes, C., and V. Vapnik, 1995, Support-vector networks: Machine learning, **20**, no. 3, 273-297.
- Demuth, H., and M. Beale, 1993, Neural network toolbox for use with MATLAB: PWS Publishing Company.
- Fung, G. M., and O. L. Mangasarian, 2005, Multicategory proximal support vector machine classifiers: Machine learning, **59**, no 1-2, 77-97.
- Gao, D., 2004, Texture model regression for effective feature discrimination: Application to seismic facies visualization and interpretation: Geophysics, **69**, 958-967.
- Gao, D., 2007, Application of three-dimensional seismic texture analysis with special reference to deep-marine facies discrimination and interpretation: An example from offshore Angola, West Africa: AAPG Bulletin, **91**, 1665-1683.
- Gao, D., 2009, 3D seismic volume visualization and interpretation: An integrated workflow with case studies: Geophysics, **74**, W1–W12.
- Gong, Q.M. and J. Zhao, 2007, Influence of rock brittleness on TBM penetration rate in Singapore granite: Tunneling and underground space technology, **22**, no.3, 317-324.
- Ghosh, K., and S. Mitra, 2009, Structural controls of fracture orientations, intensity, and connectivity, Teton anticline, Sawtooth Range, Montana: AAPG bulletin, **93**, 995-1014.
- Hall, R. J., 2016, Statistics - Introduction to Basic Concepts, <http://bobhall.tamu.edu/FiniteMath/Module8/Introduction.html>, Accessed April 14, 2016.

- Hall-Beyer, M., 2007, The GLCM Tutorial, version 2.10,  
<http://www.fp.ucalgary.ca/mhallbey/tutorial.htm>, Accessed May 9, 2016.
- Hsu, K. L., H. V. Gupta, and S. Sorooshian, 1995, Artificial neural network modeling of the rainfall-runoff process: *Water resources research*, **31**, 2517-2530.
- Johnson, K. S., and K. V. Luza, 2008, Earth sciences and mineral resources of Oklahoma, Oklahoma Geological Survey.
- Kansas Geological Survey, 2002, Paleogeomorphology of the Sub-Pennsylvanian Unconformity of the Arbuckle Group (Cambrian-Lower Ordovician),  
<http://www.kgs.ku.edu/PRS/publication/OFR2001-55/P1-04.html>, Accessed March 22, 2016.
- Koch, J. T., T. D. Frank, and T. P. Bulling, 2014, Stable-isotope chemostratigraphy as a tool to correlate complex Mississippian marine carbonate facies of the Anadarko shelf, Oklahoma and Kansas: *AAPG Bulletin*, **98**, 1071-1090.
- Lisle, R. J., 1994, Detection of zones of abnormal strains in structures using Gaussian curvature analysis: *AAPG bulletin*, **78**, 1811-1819.
- Lane, H. R., and T. L. De Keyser, 1980, Paleogeography of the late Early Mississippian (Tournaisian 3) in the central and southwestern United States, Rocky Mountain Section (SEPM).
- Lindzey, K. M., 2015, Geologically constrained seismic characterization and 3-D reservoir modeling of Mississippian reservoirs, north-central Anadarko shelf, Oklahoma: M.S. thesis, University of Oklahoma.
- Mazzullo, S. J., 2011, Mississippian Oil Reservoirs in the Southern Midcontinent: New Exploration Concepts for a Mature Reservoir Objective, v. Search and Discovery Article, p. 10373.
- Nelson, R., 2001, *Geologic analysis of naturally fractured reservoirs*: Gulf Professional Publishing.
- Northcutt, R. A., and J. A. Campbell, 1995, *Geologic provinces of Oklahoma*: Oklahoma Geological Survey.
- Qi, X., J. Snyder, T. Zhao, M. J. Pranter, and K. Marfurt, 2016, Correlation of seismic attributes and mechanical properties to rate of penetration in the Mississippian Limestone, Oklahoma, Manuscript in preparation.
- Rogers, S. M., 2001, Deposition and diagenesis of Mississippian chat reservoirs, north-central Oklahoma: *AAPG bulletin*, **85**, no. 1, 115-129.
- Seiler, M. C., and F. A. Seiler, 1989, Numerical recipes in C: the art of scientific computing: *Risk Analysis*, **9**, no. 3, 415-416.

- Wang, S. C., 2003, Artificial neural network. In *Interdisciplinary Computing in Java Programming*: Springer US.
- Watney, W. L., W. J. Guy, and A. P. Byrnes, 2001, Characterization of the Mississippian chat in south-central Kansas: *AAPG bulletin*, **85**, 85-113.
- Zhao, T., V. Jayaram, K. J. Marfurt, and H. Zhou, 2014, Lithofacies classification in Barnett Shale using proximal support vector machines: 84<sup>th</sup> Annual International Meeting of the SEG, Expanded Abstracts, 1491-1495.
- Zhao, T., S. Verma, D. Devegowda, and V. Jayaram, 2015, TOC Estimation in the Barnett Shale From Triple Combo Logs Using Support Vector Machine: 85<sup>th</sup> Annual International Meeting of the SEG, Expanded Abstracts, 791-795.
- Zuo, R., and E. J. M. Carranza, 2011, Support vector machine: a tool for mapping mineral prospectivity: *Computers & Geosciences*, **37**, no. 12, 1967-1975.

## Appendix A: Petrel – Time to Depth Conversion

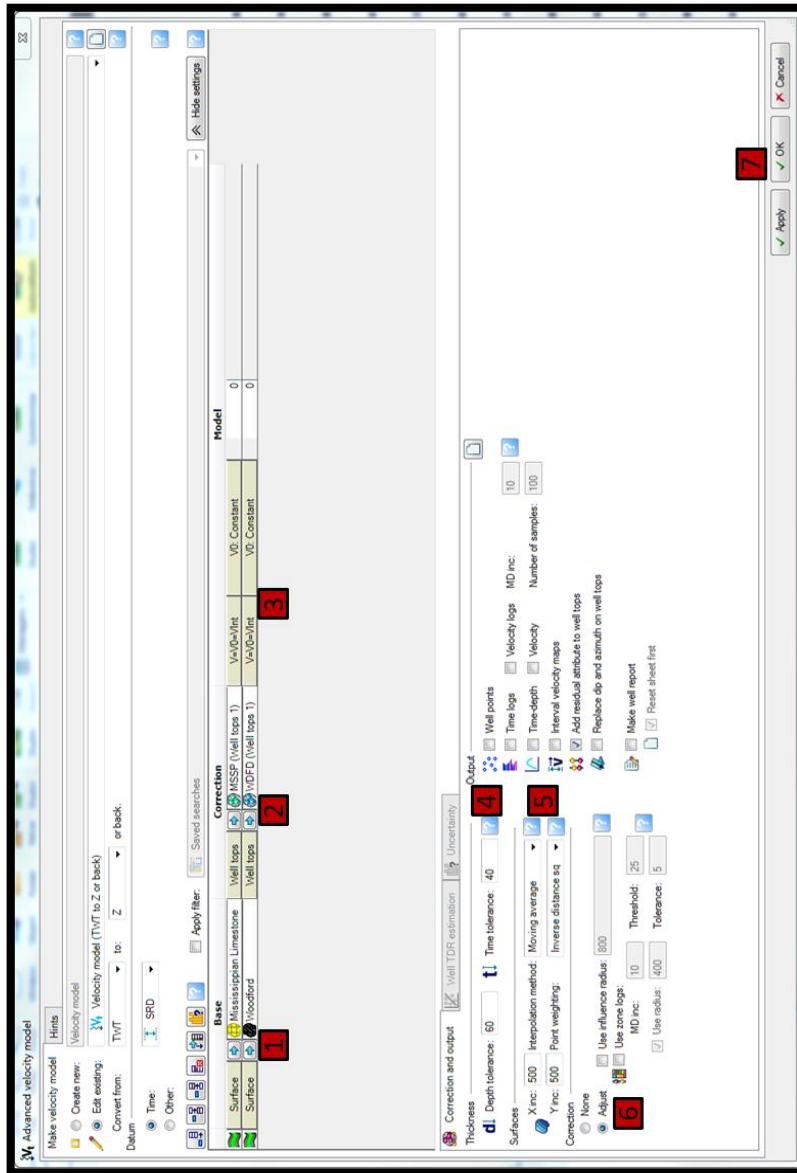


**Figure A 1.** Petrel window showing the process of how to create an advanced velocity model. 1) Insert seismic surfaces for the base. 2) Insert well tops for the correction. 3) Define the velocity model. 4) Define thickness tolerances. 5) Define interpolation method. 6) Define how the model will be corrected.

## Appendix B: AASPI – Generate Training File

1826853.74	687343.88	-3784.05	1
1826851.58	687446.56	-3823.01	1
1826853.93	687555.19	-3838.37	1
1826859.95	687665	-3840.38	1
1826866.33	687774.77	-3843.52	1
1826872.57	687884.56	-3845.66	1
1826877.66	687994.4	-3842.92	1
1826878.47	688104.33	-3839.93	1
1826876.32	688214.3	-3840.97	1
1826873.85	688324.25	-3843.02	1
1826871.34	688434.22	-3843.96	1
1826869.35	688544.19	-3842.72	1
1826867.12	688654.13	-3839.55	1
1826864.03	688764.07	-3837.82	1
1826859.64	688873.98	-3837.42	1
1826855.39	688983.9	-3836.49	1
1826851.36	689093.81	-3834.71	1
1826847.36	689203.73	-3833.35	1
1826844.81	689313.7	-3832.63	1
1826845.35	689423.68	-3831.11	1
1826848.39	689533.62	-3829.23	1
1826851.99	689643.56	-3828.46	1
1826854.88	689753.52	-3827.27	1
1826857.71	689863.48	-3826.45	1
1826859.91	689973.46	-3825.71	1
1826860.69	690083.45	-3825.52	1
1826859.42	690193.44	-3825.16	1
1826858	690303.44	-3824.75	1
1826857	690413.43	-3824.22	1
1826856.63	690523.43	-3823.16	1
1826856.7	690633.43	-3822.39	1
1826856.32	690743.41	-3820.46	1
1826855.9	690853.37	-3817.42	1
1826854.97	690963.3	-3813.58	1
1826853.12	691073.2	-3809.31	1
1826851.07	691183.11	-3805.32	1
1826848.87	691293.02	-3801.34	1
1806074.95	703103.75	-3651.51	2
1806080.23	703212.72	-3664.28	2
1806084.94	703322.61	-3665.4	2
1806089.77	703432.5	-3664.85	2
1806094.31	703542.39	-3664.9	2
1806096.57	703652.33	-3667.25	2
1806098.01	703762.25	-3663.67	2
1806099.19	703872.22	-3661.99	2
1806100.51	703982.22	-3662.23	2
1806101.66	704092.21	-3661.96	2

**Figure A 2.** A sample input well path file for the AASPI Generate Training File program. Column 1 corresponds to the X coordinates. Column 2 corresponds to the Y coordinates. Column 3 corresponds to the Z coordinate. Column 4 corresponds to the well number.

5.30064964	0.00000649	-0.00002412	19.92660332	23.23864365	19242.07812500	1
3.98776674	0.00003202	-0.00001383	42.22288895	52.40589905	39466.98828125	1
4.25733137	0.00005252	-0.00001205	37.64720917	44.68894958	36854.62500000	1
3.92470336	0.00004006	-0.00001410	39.87992096	49.94456100	38688.62109375	1
3.76442242	0.00013533	-0.00001652	46.45366669	43.45014954	37754.21093750	1
4.53472853	0.00004619	-0.00001271	40.16915131	62.76888275	41939.94531250	1
4.15953636	0.00004544	-0.00019829	38.84847260	46.77622604	37736.79687500	1
3.46088886	0.00001313	-0.00006144	40.10825729	30.46758270	32890.55078125	1
3.42214704	0.00008592	-0.00004983	39.98212433	45.27419281	36793.22656250	1
3.38548374	0.00002003	-0.00003541	39.96343613	36.15473557	34552.02343750	1
3.36603093	0.00004420	-0.00000763	24.27015305	17.93516541	19342.53320312	1
3.36842918	0.00000320	-0.00003511	19.20298004	11.81979370	15407.50976562	1
3.39321280	0.00004176	-0.00008704	19.27039719	12.94020537	15769.93457031	1
3.40597248	0.00003418	-0.00003202	35.82022095	30.59718895	30499.03515625	1
3.39566612	0.00000575	-0.00002307	21.61027336	19.94732285	20293.43554688	1
3.39607096	0.00000111	-0.00002119	17.96881676	17.50300026	16621.07617188	1
3.38995147	0.00002803	-0.00014113	42.80359650	40.11868668	32618.84375000	1
3.37688780	0.00002510	-0.00011117	40.61742401	37.59307480	34539.76562500	1
3.36002207	0.00008755	-0.00014297	32.93798065	29.97253036	31452.75781250	1
3.35114670	0.00007978	-0.00010551	41.02380371	50.62543488	38495.49218750	1
3.35713053	0.00002299	-0.00002381	41.88037109	54.26789093	39814.83593750	1
3.36418438	0.00002995	-0.00001097	38.68943024	44.60488892	37056.24218750	1
3.39703989	0.00004792	-0.00010022	44.32722473	40.26551819	36571.48828125	1
3.42004919	0.00006342	-0.00007798	41.44715118	52.41900635	39507.54687500	1
3.43101978	0.00007082	-0.00004910	37.96696472	77.53491974	45047.10937500	1
3.42182159	0.00004768	-0.00004107	39.09505081	55.75143814	39357.41406250	1
4.41034293	0.00000090	-0.00005322	38.16582108	34.74153137	33809.75390625	1
3.40715075	0.00000805	-0.00006965	40.07424927	42.26329803	36032.91406250	1
3.40709448	0.00009468	-0.00006733	44.72991943	38.98822403	35945.31250000	1
3.42436838	0.00006136	-0.00003149	30.13012695	20.36404037	23187.72070312	1
3.58694100	0.00000529	-0.00000914	18.59731102	11.50165367	15115.28222656	1
3.89381718	0.00000390	-0.00001099	19.19662285	12.98633003	15720.74804688	1
3.97693300	0.00000768	-0.00000698	19.00784111	19.81016350	17649.53125000	1
3.90867901	0.00002779	-0.00000581	17.85845566	20.60534477	17571.40234375	1
3.97822642	0.00004836	-0.00001417	19.32777405	18.09620094	17124.29101562	1
4.24785137	0.00002906	-0.00005033	30.34845352	41.17798233	29721.47265625	1
4.65513945	0.00000228	-0.00007045	36.30726242	48.69564056	37330.13281250	1
5.76913261	-0.00001584	-0.00010366	38.93412399	53.90245056	39586.85156250	2
5.08219051	0.00001054	-0.00007900	37.41194153	50.3188965	38458.46875000	2
5.19445753	0.00005949	-0.00000180	39.43675995	54.22332764	39902.85156250	2
5.35744190	0.00005176	-0.00001715	39.33733688	55.75967407	40289.79687500	2
5.08437347	-0.00000172	-0.00005792	37.54501343	43.57864380	36579.13671875	2
4.75462627	0.00004576	-0.00001309	37.16233444	38.66822052	34815.97656250	2
4.99592161	0.00000083	-0.00007257	39.50188446	37.03659821	34406.91406250	2
5.05901337	0.00001440	-0.00001809	38.61925888	32.54703522	33229.69921875	2
4.99142456	0.00000127	-0.00001387	14.85146999	9.49345398	12143.12597656	2
5.20312881	0.00003704	-0.00000284	22.21689224	19.73146820	19809.84179688	2
5.30567932	0.00004032	-0.00004001	36.73806000	40.15357971	34967.36718750	2
5.28026056	0.00002301	-0.00000090	24.68889618	31.70503616	24801.28320312	2
5.33096886	0.00000181	-0.00003122	23.72334480	27.01618767	22852.56250000	2
5.15953541	0.00008472	-0.00000939	32.98167953	34.53219604	32176.19531250	2
5.15240049	0.00003265	-0.00001380	39.50788879	50.08804321	38583.16406250	2
5.12057829	0.00001995	-0.00001418	40.53171539	55.25986481	40152.73437500	2
5.36633205	0.00001921	-0.00001937	31.86429787	28.99834061	30534.57031250	2
5.39134359	-0.00000562	-0.00007640	35.78742599	58.62365723	40222.62500000	2
5.88492012	0.00000627	-0.00003151	41.02923584	60.16811371	41577.60156250	2
5.96686840	0.00003331	-0.00002966	37.91510773	55.67502975	39930.25000000	2
6.23055315	0.00006183	-0.00001312	39.56903076	39.56903076	39966.90234375	2
6.27935696	-0.00001904	-0.00007293	39.34635925	59.21543121	41126.56640625	2
5.89832640	0.00002618	-0.00001551	41.13487625	59.28740692	41321.19140625	2
5.59237003	0.00000081	-0.00006081	38.11897388	42.93080902	36333.64843750	2
5.67664909	0.00004028	-0.00005011	36.49868774	30.53863525	32149.63671875	2
5.53873396	0.00006290	-0.00003203	39.53560257	40.52309265	35137.90234375	2
5.46339512	0.00004161	-0.00000213	38.60312653	31.38107491	32991.97265625	2
4.94367599	0.00001472	-0.00001488	16.73046494	12.40272331	14184.08886719	2
4.61281157	0.00003399	-0.00003330	33.27459717	35.64449692	31809.72265625	2
4.68551445	0.00003412	-0.00000408	37.38875580	41.20976257	35646.78125000	2
4.82635784	0.00001968	-0.00003539	27.08851814	31.94961166	26299.53710938	2
4.77464390	0.00000038	-0.00007659	16.39320564	14.34871769	16997.87695312	2
4.79511690	0.00000214	-0.00004256	33.33964920	49.39965439	34059.56640625	2
4.76899147	0.00002791	-0.00001886	41.77083206	56.17040634	40463.20312500	2
4.69190979	0.00004874	0.00000121	37.63370895	40.25542450	35519.82421875	2
4.71998930	0.00008083	0.00000835	32.03402328	27.82876778	30522.58789062	2
5.04310513	0.00003675	-0.00001466	37.69886017	40.86277008	35558.57812500	2
5.27448416	0.00005641	-0.00001101	36.72830963	38.68768311	34753.07421875	2
5.45845127	0.00001983	-0.00004343	37.85982132	53.24945068	39089.19140625	2
4.95938301	0.00003951	-0.00004931	37.83252716	47.39429092	37560.27734375	2
4.94701815	0.00003463	-0.00002374	36.04987335	57.96180725	40170.73828125	2

**Figure A 3.** A sample output file from the AASPI Generate Training File program. Column 1 through 6 corresponds to the extracted geometric and geomechanical attributes. Column 7 is the well number of each point.

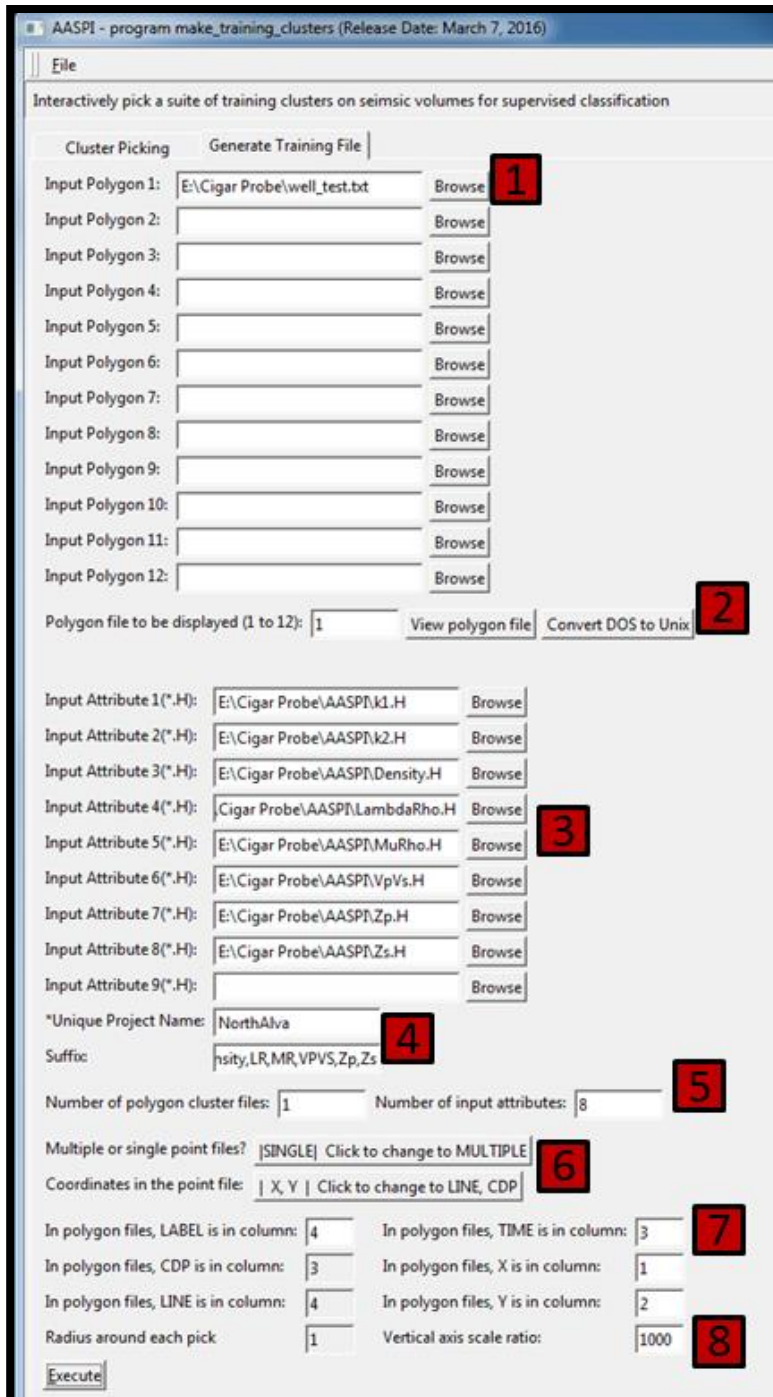


**Figure A 4.** AASPI window showing the inputs and settings for the Generate Training File program. 1) Input well path file. 2) Choose the amount of well path files to use. 3) Insert the AASPI format 3D seismic volumes to have values extracted. 4) Give the output a filename. 5) Choose the number of input attributes. 6) Change point file to “SINGLE” and coordinates to “X,Y”. 7) Change values to correspond with their respective columns. 8) Change the vertical axis scale ratio to match the data.

## Appendix C: AASPI – PSVM Welllogs

Porosity	Curvedness	LR	MR	Zp	Class	
6.56495571	3.51E-05	39.65456772	50.92187119	39040.125		1
6.80943203	4.01E-05	36.84760284	52.54854202	38696.03906		2
5.30818653	3.24E-05	38.02157593	51.00726318	38549.55469		1
5.30610609	3.30E-05	44.41124725	49.00592804	38920.38281		2
5.4274044	2.62E-05	53.0147934	45.14680481	39084.20313		1
5.50149345	4.64E-05	41.69501495	54.2892189	40107.12891		1
5.51593971	6.49E-05	40.23519135	63.09860229	42211.82031		1
5.73889732	3.66E-05	39.62538147	61.35032272	41780.00781		2
5.62603283	1.94E-05	38.31437683	47.01576233	37705.70313		2
5.67691994	2.11E-05	39.82867432	30.19813347	32768.02344		1
5.80524158	2.69E-05	41.09545517	33.35551453	33658.66016		1
5.89804649	3.64E-05	39.9889679	34.90312958	34141.89844		1
5.6568861	3.14E-05	26.31309128	20.15510559	22125.53711		2
5.60686922	2.07E-05	44.53142929	52.13999939	39519.49219		2
5.48581409	3.30E-05	41.72026062	48.41295624	38375.77344		2
5.32234955	2.53E-05	37.10244751	38.31884384	34954.63281		1
5.40377522	3.79E-05	38.29949188	43.05760193	36564.98438		1
5.27405691	8.27E-05	37.20510101	47.21269989	37604.96875		1
5.14859533	3.52E-05	37.6674881	92.90206909	48377.61719		2
5.05835533	7.01E-05	41.62443542	47.26384735	37559.89453		1
4.96620083	4.41E-05	39.27134705	37.09128571	34535.92578		1
5.11258602	3.70E-05	40.03457642	34.15407562	34366.54297		1
5.23020411	2.72E-05	40.25521088	35.37184143	34501.85938		1
5.29252148	2.67E-05	19.39978409	13.28970242	16052.56445		2
5.32848263	3.22E-06	17.82202721	11.09734631	14471.85547		2
5.3602581	5.02E-05	38.30978012	34.6048584	33145.375		2
5.31104469	3.15E-05	21.11671257	23.75973129	20072.39258		1
5.21419334	2.12E-05	16.37385368	19.51022148	17544.07227		2
5.12170601	4.34E-05	32.99009323	31.87964439	32219.64844		2
5.26492596	0.000106096	37.68355942	39.83054352	35342.19531		2
5.42189407	4.67E-05	40.07480621	59.33811188	41081.10547		1
5.68288136	6.57E-05	38.87952042	53.35803604	39459.33594		1
5.89080906	2.69E-05	40.68300247	47.26581573	38110.96484		1
5.89882469	3.26E-05	39.89983368	51.17838287	39099.82813		1
5.69300365	3.46E-05	42.37667084	54.45101166	40337.16406		1
2.70977163	3.72E-05	40.63347244	54.16940308	39983.83594		1
5.94221687	3.03E-05	38.73390961	46.40885925	37713.14063		1
9.49766731	3.25E-05	35.3489151	35.28047562	33673.27344		1
6.34712601	3.29E-05	35.59173584	38.70409012	34825.9375		1
7.29908228	3.49E-05	39.73114777	70.23806763	43478.15625		1
3.92065716	4.50E-05	37.1062355	44.1711731	36602.10156		1
6.79483223	4.22E-05	22.86280441	21.79943085	23136.54102		2
6.78514147	2.74E-06	3.61305809	3.98911214	3345.436523		1
5.29190922	2.34E-05	21.78354073	20.53117943	20291.19141		2
5.48097992	2.78E-06	1.61764264	1.38872683	1575.843018		1
5.68079853	1.53E-05	24.63747978	13.39109993	17716.58203		1
4.84243774	1.54E-05	29.86405373	19.08909035	23774.38867		2
3.23760676	2.26E-05	35.19823456	32.96055222	31417.22852		2
3.91111302	3.31E-05	39.38546371	40.94643402	35959.42188		2
4.27895975	4.93E-05	38.98844528	46.18271637	37357.49609		2
4.56762123	2.43E-05	39.01462173	45.44050217	37178.17969		1
4.63461685	9.87E-06	54.28926086	49.56069946	40320.43359		2
4.45298195	2.98E-05	49.29312515	54.27125549	41078.42969		2
4.34650421	3.77E-05	38.83963776	51.24954224	38820.39453		2
4.61195564	5.02E-05	37.3981514	42.32215881	36041.51953		1
5.28023958	2.85E-05	36.70796967	25.91266823	28703.46875		2
5.29591703	3.64E-05	31.19310951	18.63003159	24138.09375		1
5.170825	4.10E-05	34.48175812	25.5123291	29061.55859		1
5.1158843	2.68E-05	38.84073639	38.16072845	35027.40234		1
5.27257967	6.61E-05	48.95862579	39.63868713	36888.85547		2
5.42521763	5.49E-05	44.41637802	43.71666718	37409.60156		2
5.74245071	3.76E-05	44.82409668	42.26101303	37213.37891		2
6.16789818	1.98E-05	42.4344902	49.85801697	38843.03125		2
6.34677172	1.84E-05	38.79706192	51.48247528	38950.53125		2
6.21063948	3.86E-05	37.26685333	53.49143982	39289.67188		2
6.17021418	0.000116008	44.34501648	42.85333633	37141.32031		2
6.4849391	7.09E-05	42.63181305	37.83164215	35450.19141		2
6.38023329	3.94E-05	44.64889526	55.92641068	40710.30078		2
6.03867292	5.31E-05	36.18516922	37.49900436	33322.15234		2

**Figure A 5.** Sample PSVM training data. The first five columns represent input geomechanical and geometric attributes, while column 6 is the defined class of the well – in this case, high or low COP.

Porosity	Curvedness	LR	MR	Zp	Class	
5.6904583	2.45E-05	18.06006622		11.2859211	14757.60254	1
5.82866669	2.65E-05	31.1836319		29.14260101	28021.19531	2
5.57429504	3.28E-05	39.63739777		33.84627151	33565.73047	2
5.22154951	2.32E-05	20.92841721		16.97684479	18900.97266	2
5.07056141	2.52E-05	20.14515495		19.9246006	17867.64648	2
4.99498081	5.40E-05	37.19315338		46.32849884	34819.17969	1
5.10396147	4.43E-05	38.60116577		45.41955566	37281.18359	1
5.46157265	1.82E-05	34.7842865		31.69504547	32436.95898	2
4.96321392	5.48E-05	38.87738419		35.02817535	34072.29297	1
4.88985348	2.25E-05	42.27478409		48.02820969	38260.30078	1
5.03214741	3.61E-05	43.06558228		39.09980392	35797.60938	2
5.21790838	3.65E-05	29.40742111		20.40594673	26835.9082	2
5.54135704	2.58E-05	33.85336304		40.69395447	34414.84766	2
5.7552104	8.08E-06	16.9744339		21.44748497	17142.82422	2
5.65832424	9.64E-06	9.45324707		8.14531326	7541.780273	2
5.46528149	2.21E-05	29.09370995		25.52048874	24812.06641	1
3.26669407	2.28E-05	25.0766716		18.76497078	21115.67773	1
3.17988253	3.40E-05	38.4415741		36.28738022	34079.58984	2
3.13935947	2.14E-05	38.84853363		42.71669006	35737.95313	1
2.96778631	3.76E-05	39.8285141		36.48823547	34575.80078	2
3.00665474	0.000104919	47.65122604		45.15362167	38127.24219	1
3.07067108	3.22E-05	42.84438705		77.57409668	45908.92969	1
3.10006523	2.45E-05	39.82709122		48.88256073	38331.48047	2
2.9848752	2.24E-05	37.30276489		51.7238884	38761.95703	1
5.25163269	2.43E-05	42.59994507		42.49676895	36869.10547	2
4.43361473	4.40E-05	45.38073349		48.76399231	38837.46875	2
3.91254926	1.90E-05	57.35567474		54.24178314	41661.67578	2
3.64014864	3.43E-05	37.75387192		31.41906548	32655.75391	1
3.59928751	2.73E-05	31.84880829		19.08310699	25687.39453	1
3.50777078	6.19E-05	41.87876129		32.14951324	33442.60156	1
3.49334645	6.79E-05	32.95717621		20.10925102	26196.64063	1
3.49865484	2.80E-05	31.63098526		18.24483681	25249.26367	1
5.5394659	3.43E-05	61.96512604		79.44598389	48546.92188	2
5.75691175	2.74E-05	44.5045166		64.85276794	42944.5	1
5.99447155	2.93E-05	37.45478058		51.35670471	38665.20313	1
5.89102602	5.95E-05	36.57868958		41.81537628	35666.61719	1
5.64175367	7.38E-05	48.2319603		43.19086456	37855.96094	2
5.48952818	4.18E-05	46.02563477		53.96963882	40685.28125	2
5.56992245	3.04E-05	44.13983536		42.43865204	37155.80859	2
5.67767429	1.49E-05	31.83831406		25.07796097	29124.92969	2

**Figure A 6.** Sample PSVM testing data. The first five columns represent input geomechanical and geometric attributes to be tested with the model created from the inputs. Column 6 is compared to the testing outputs created from the training model.

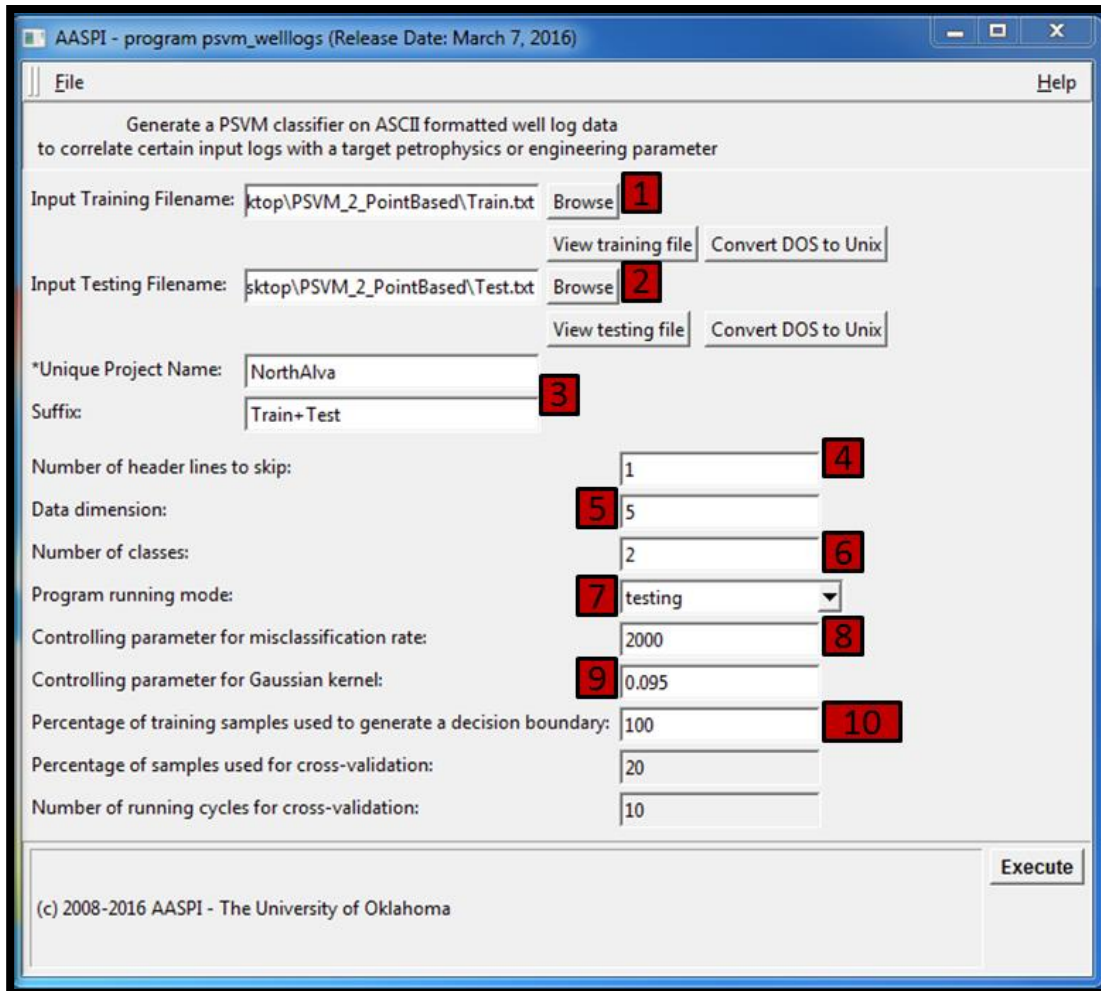


**Figure A 7.** AASPI window showing the inputs and settings for a PSVM test. 1) Enter the training points. 2) Enter the testing points. 3) Name the output file. 4) Skip header lines. 5) Choose the number of input variables. 6) Choose the number of classes. 7) Pick the testing mode. 8) Define the parameter for misclassification. 9) Define the Gaussian kernel parameter. 10) Choose the number of samples to use when generating the decision boundary.

## Appendix D: MATLAB – Artificial Neural Network Inputs

4.75462627	2.66965E-05	37.16233444	38.66822052	34815.97656
4.7199893	1.50269E-05	32.03402328	27.82876778	30522.58789
5.15240049	5.63751E-05	39.50788879	50.08804321	38583.16406
5.04310513	1.56151E-05	37.69886017	40.86277008	35558.57813
5.76913261	3.04133E-05	38.93412399	53.90245056	39586.85156
4.69190979	0.000100434	37.63370895	40.2554245	35519.82422
5.15953541	4.37237E-05	32.38167953	34.53219604	32176.19531
5.12057829	7.78808E-05	40.53171539	55.25986481	40152.73438
5.36633205	0.000100163	31.86429787	28.99834061	30534.57031
5.33096886	2.03915E-05	23.7233448	27.01618767	22852.5625
5.27448416	2.88748E-05	36.72830963	38.68768311	34753.07422
4.95938301	3.10933E-05	37.83252716	47.39429092	37560.27734
5.08437347	3.76574E-05	37.54501343	43.5786438	36579.13672
5.8983264	1.32627E-05	41.13487625	59.28740692	41321.19141
4.94367599	2.2124E-05	16.73046494	12.40272331	14184.08887
5.19445753	8.32167E-05	39.43675995	54.22332764	39902.85156
5.45845127	2.4975E-05	37.85982132	53.24945068	39089.19141
4.7951169	5.2968E-05	33.3396492	49.39965439	34059.56641
4.94701815	2.83455E-05	36.04987335	57.96180725	40170.73828
5.59237003	5.45372E-05	38.11697388	42.93080902	36333.64844
4.76899147	3.93237E-05	41.77083206	56.17040634	40463.20313
6.27935696	2.51141E-05	39.34635925	59.21543121	41126.56641
5.3574419	2.62324E-05	39.33733368	55.75967407	40289.79688
5.67664909	4.30203E-05	36.49868774	30.53863525	32149.63672
4.61281157	2.29303E-05	33.27459717	35.64449692	31809.72266
4.7746439	3.70594E-05	16.39320564	14.34871769	16997.87695
4.68551445	5.71994E-05	37.3887558	41.20976257	35646.78125
5.88492012	3.22426E-05	41.02923584	60.16811371	41577.60156
5.46339512	2.87793E-05	38.60312653	31.38107491	32991.97266
5.28026056	1.71176E-05	24.68889618	31.70503616	24801.2832
4.99142456	2.60957E-05	14.85146999	9.49345398	12143.12598
5.39134359	7.87566E-05	35.78742599	58.62365723	40222.625
6.23055315	1.34448E-05	39.56903076	55.12878036	39966.90234
4.82635784	5.5582E-05	27.08851814	31.94961166	26299.53711
5.08219051	2.4455E-05	37.41194153	50.31188965	38458.46875
5.9668684	3.06659E-05	37.91510773	55.67502975	39930.25
5.20312881	7.13054E-05	22.21689224	19.7314682	19809.8418
5.05901337	6.57681E-05	38.61925888	32.54703522	33229.69922
4.99592161	5.64603E-05	39.50188446	37.03659821	34406.91406
5.30567932	1.62793E-05	36.73806	40.15357971	34967.36719
5.53873396	6.72529E-05	39.53560257	40.12309265	35137.90234
5.88816786	2.46632E-05	38.4657402	47.64693832	37828.96484
9.43953514	3.81022E-05	39.99207306	50.27039337	38783.20313
5.20593309	7.18596E-05	38.92475128	37.14530563	34792.04688
8.00834846	2.91862E-05	38.61435699	50.57054138	38519.24609
6.64570808	3.3758E-05	37.65163803	52.29262924	39063.1875
7.15505028	4.15104E-05	40.66156387	57.53287888	40741.47266
5.31360579	1.55541E-05	33.88444138	26.26993179	28927.51953
5.43874454	3.45369E-05	5.38159275	6.31899405	5229.023926
5.19782972	6.72878E-05	27.97084999	36.37742233	28219.75781
5.34178638	3.33948E-05	5.49972153	5.26645803	4516.538086
5.22897434	6.57285E-05	40.04299927	50.19681931	38706.14844
5.23261118	2.68711E-05	40.20214462	44.28091812	37149.98438
5.10635662	0.000122536	37.94367218	52.94870758	39035.06641
5.08593941	9.60922E-05	36.44174576	29.9290657	32176.85156
4.65526581	6.05767E-05	4.56622744	3.55095816	4228.158203
5.59826851	2.61187E-05	32.24768448	20.9130764	26426.38672

**Figure A 8.** Sample ANN input values. Columns 1 through 5 represent input geometric and geomechanical values.

